A Polynomial-Time Algorithm for Computing a Shortest Path of Bounded Curvature Amidst Moderate Obstacles

Jean-Daniel Boissonnat, Sylvain Lazard

INRIA

INSTITUT NATIONAL DE RECHERCHE EN INFORMATIQUE ET EN AUTOMATIQUE

A polynomial-time algorithm for computing a shortest path of bounded curvature amidst moderate obstacles

Jean-Daniel Boissonnat , Sylvain Lazard

N° 2887

mai 1996

THÈME 2

ISSN 0249-6399

INRIA
SOPHIA ANTIPOLIS

A polynomial-time algorithm for computing a shortest path of bounded curvature amidst moderate obstacles

Jean-Daniel Boissonnat , Sylvain Lazard

Thème 2 — Génie logiciel
et calcul symbolique
Projet Prisme

Rapport de recherche n ° 2887 — mai 1996 — 45 pages

Abstract: In this paper, we consider the problem of computing a shortest path of bounded curvature amidst obstacles in the plane. More precisely, given prescribed initial and final configurations (i.e. positions and orientations) and a set of obstacles in the plane, we want to compute a shortest C^1 path joining those two configurations, avoiding the obstacles, and with the further constraint that, on each C^2 piece, the radius of curvature is at least 1. In this paper, we consider the case of moderate obstacles (as introduced by Agarwal et al.) and present a polynomial-time exact algorithm to solve this problem.

Key-words: Non-holonomic robot, motion planning, shortest paths, mobile robot, computational geometry.

(Résumé : tsvp)

Unité de recherche INRIA Sophia-Antipolis
2004 route des Lucioles, BP 93, 06902 SOPHIA-ANTIPOLIS Cedex (France)
Téléphone : (33) 93 65 77 77 – Télécopie : (33) 93 65 77 65

Algorithme polynomial pour le calcul d'un plus court chemin de courbure bornée en présence d'obstacles modérés

Résumé : Nous nous intéressons au problème du calcul d'un plus court chemin de courbure bornée en présence d'obstacles dans le plan. Plus précisement, étant donné des configurations (i.e. positions et orientations) initiale et terminale, et un ensemble d'obstacles dans le plan, nous voulons calculer un plus court chemin C^1 joignant ces deux configurations, évitant les obstacles et tel que que la courbure de la trajectoire soit majorée par 1 en tout point où elle est définie. Dans ce papier, nous considérons le cas d'obstacles modérés (introduits par Agarwal et al.) et présentons un algorithme exact polynomial pour résoudre ce problème.

Mots-clé : Système mécanique non holonome, planification de trajectoires, plus courts chemins, robotique mobile, géométrie algorithmique.

1 Introduction

In this paper, we consider the problem of computing a shortest path of bounded curvature amidst obstacles in the plane, SBC path for short. More precisely, given prescribed initial and final configurations (i.e. positions and orientations) and a set of obstacles in the plane, we want to compute a shortest C^1 path joining those two configurations, avoiding the obstacles, and with the further constraint that, on each C^2 piece[1], the radius of curvature is at least 1. This question appears in many applications and goes back to Markov who studied the problem for joining pieces of railways. More recently, a great deal of attention has been paid to this question in the context of non-holonomic robot motion planning [2, 14, 15, 16]. A robot is said to be non-holonomic if some kinematics constraints locally restricts the authorized directions for its velocity. A typical non-holonomic robot is a car : assuming no slipping of the wheels on the ground, the velocity of the midpoint between the two rear wheels of the car is always tangent to the car axis. Though the problem considered in this paper is one of the simplest instances of non-holonomic motion planning, it is still far from being well understood.

Even in the absence of obstacles, the problem is not easy. Dubins [10] proved that any SBC path takes one of the following forms CSC or CCC, where C means a circular arc of radius 1 and S a straight line segment. The proof in Dubins paper is quite long and intricate. Recently, a much simpler proof has been obtained using the Minimum Principle of Pontryagin (a central result in Control Theory) [5, 18] and a complete characterization of SBC paths has also been established [7].

The problem becomes much harder in the presence of obstacles. By basic theorems in Control Theory, there exists a SBC path amidst obstacles and joining two given configurations as soon as there exists a BC path, i.e. a (not necessarily optimal) C^1 path joining the two given configurations, avoiding the obstacles and where the radius of curvature is everywhere (where it is defined) greater of equal to 1. Moreover, a SBC path is a finite concatenation of subpaths either contained in the boundary of some obstacle or joining two obstacle edges (considering the initial and the final configurations as point obstacles); each subpath joining two obstacle edges is a Dubins path, i.e. a path of type CSC or CCC. Computing a shortest path seems however a formidable task. Even if we remove the requirement for the path to be a shortest one and look for a BC path (instead of a SBC path), no polynomial-time algorithm is known. In [11], Fortune and Wilfong present an exact algorithm that can decide if a BC path exists but does not generate the path in question. This

[1] As we will see below, the optimal path is piecewise C^2.

algorithm runs in time and space that is exponential with respect to the number n of corners of the environment and the number of bits used to specify the positions of the corners. By the remark above, this algorithm can also decide if a SBC path exists.

For computing SBC paths, only approximate algorithms have been proposed in the literature. Jacobs and Canny [12] discretize the problem and calculate a path that approximates the shortest one in time $O(n^2(\frac{n+L}{\varepsilon})\log n + \frac{(n+L)^2}{\varepsilon^2})$, where ε describes the closeness of the approximation and L is the total edge length of the obstacle boundaries. Very recently, Wang and Agarwal [19] improved on this result and proposed an algorithm whose time complexity is $O(\frac{n^2}{\varepsilon^2}\log n)$, and thus does not depend on L. In another recent paper, Agarwal et al. [1] have considered a restricted class of obstacles, the so-called moderate obstacles : an obstacle is said to be moderate if it is convex and if its boundary is a differentiable curve whose radius of curvature is everywhere greater or equal to 1. This restriction is quite strong but valid in many practical situations. Under the assumption that all the obstacles are disjoint and moderate, Agarwal et al. show that an approximate SBC path can be computed in $O(n^2 \log n + 1/\varepsilon)$ time.

In this paper, we consider also the case of moderate obstacles (in a more restrictive sense than Agarwal et al.) and present a polynomial-time algorithm to compute a SBC path (assuming that the roots of some polynomials of bounded degree can be computed in constant time). To the best of our knowledge, this is the first polynomial-time exact algorithm for a non trivial instance of the problem.

The paper is organized as follows. In Section 2, we introduce some notations and show that the problem reduces to finding an Euclidean shortest path when the initial and the final positions are sufficiently far away and also sufficiently far from the obstacles. In the following Sections 3, 4 and 5 we show that SBC paths belong to a finite family. In Section 6, we describe an algorithm that computes an optimal path between two given configurations.

2 Preliminaries

First, we give some definitions and notations. Let Ω be a set of obstacles. In this paper, the obstacles are assumed to be disjoint and moderate. An obstacle is said to be *moderate* if it is convex and if its boundary is a differentiable curve made of line segments and circular arcs of unit radius. For convenience and without real loss of generality, we assume that no two edges of the obstacles are parallel. A path that

avoids the obstacles (i.e. that does not intersect the interior of the obstacles) is called *free*. In the sequel, a free SBC path is simply called an *optimal path*.

Let $\omega_S = (S, \vec{U}_S)$ and $\omega_T = (T, \vec{U}_T)$ be two configurations (i.e. positions and orientations). Let $\mathcal{P}$ be an optimal path joining ω_S to ω_T. As mentioned in the introduction, $\mathcal{P}$ is a finite concatenation of O, C and S-segments; an O-segment is a maximal portion of $\mathcal{P}$ that coincides with the boundary of an obstacle; a C-segment is a maximal circular arc of unit radius that is not an O-segment; a S-segment is a maximal line segment, possibly on the boundary of some obstacle. To a path, we will associate the sequence of the types (O, C or S) of its segments.

The first and last segments are called *terminal*. A terminal segment is, in general, a C-segment; we denote it by C_t. A C-segment (or a circle of unit radius) is denoted by $\bar{C}$ if it is tangent to at least one obstacle. A C-segment (or a circle of unit radius) is called *anchored* and denoted by $\bar{\bar{C}}$ either if it is tangent to at least two obstacles, or if it is tangent to at least one obstacle and adjacent to a terminal C-segment, or if it is terminal.

The first theorem shows that, when the initial and the final positions are sufficiently far away and also sufficiently far from the obstacles, the optimal path is an Euclidean shortest path for an augmented set of obstacles.

Let M be a point of $\mathcal{P}$ and let $C_L(M)$ (resp. $C_R(M)$) be the unit circle tangent to $\mathcal{P}$ at M and lying on the left (resp. right) side of the path $\mathcal{P}$ oriented from S to T. $C_L(M)$ is oriented counterclockwise and $C_R(M)$ is oriented clockwise. An arc of one of these circles will be oriented accordingly.

Let C'_S (resp. C'_T) be the circle tangent to $C_L(S)$ and $C_R(S)$ ($C_L(T)$ and $C_R(T)$) that does not intersect the ray $(S, \vec{U}_S)$ (the ray $(T, -\vec{U}_T)$) (see Figure 1). Let $\mathcal{R}_S$ (resp. $\mathcal{R}_T$) be the shaded region limited by $C_L(S)$, $C_R(S)$ and C'_S ($C_L(T)$, $C_R(T)$ and C'_T) in Figure 1.

Lemma 1 *If $\mathcal{R}_S$ and $\mathcal{R}_T$ are disjoint and do not intersect the obstacles, $\mathcal{P}$ does not intersect the interior of $\mathcal{R}_S$ nor that of $\mathcal{R}_T$.*

Proof: We assume for a contradiction that $\mathcal{P}$ intersects the interior of $\mathcal{R}_S$. We consider first the case where $\mathcal{P}$ does not intersect the interior of $\mathcal{R}_T$. As $\mathcal{P}$ is a path of bounded curvature, $\mathcal{P}$ intersects $C_L(S)$ or $C_R(S)$. Let I be the last intersection point (along $\mathcal{P}$) between $\mathcal{P}$ and $C_L(S) \cup C_R(S)$; we assume, without loss of generality, that $I \in C_L(S)$. Let I' be the last intersection point (along $\mathcal{P}$) between $\mathcal{P}$ and $\mathcal{R}_S$ and let II' be the part of $\mathcal{P}$ from I to I'. We denote by A the point common to $C_L(S)$ and C'_S (see Figure 1).

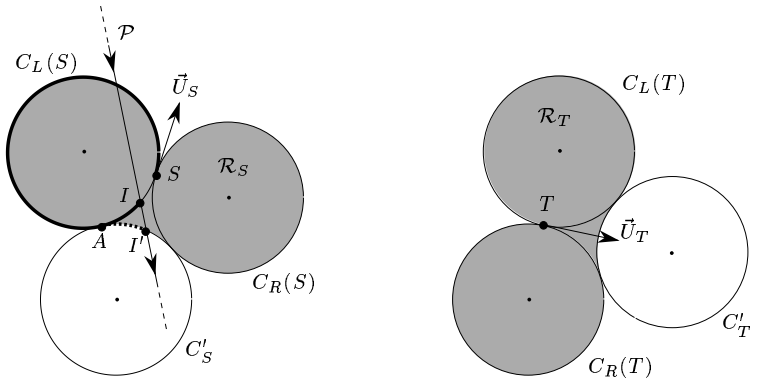

Figure 1: Regions $\mathcal{R}_S$ and $\mathcal{R}_T$

First, we assume that $I \neq S$. Let SI be the arc of $C_L(S)$, oriented as $C_L(S)$, that starts at S and ends at I. Let $\mathcal{P}'$ be the concatenation of SI and the part of $\mathcal{P}$ from I to T. $\mathcal{P}'$ is not a path of bounded curvature but it is shorter than $\mathcal{P}$ since the shortest path of bounded curvature from ω_S to I (the orientation at I is not specified) is the arc SI [4]. Let $\mathcal{P}''$ be the path obtained by modifying $\mathcal{P}'$ as follows : if $I' \neq I$, then we replace the arc AI of $C_L(S)$ and II' by the circular arc AI' of C'_S. The path $\mathcal{P}''$ is shorter than $\mathcal{P}'$. Thus $\mathcal{P}''$ is shorter than $\mathcal{P}$, avoids all the moderate obstacles, avoids $\mathcal{R}_S$ by construction and $\mathcal{R}_T$ because $\mathcal{R}_S \cap \mathcal{R}_T = \emptyset$. Hence, the Euclidean shortest path from S to T avoiding Ω, $\mathcal{R}_S$ and $\mathcal{R}_T$ is shorter than $\mathcal{P}$. That yields a contradiction because this Euclidean shortest path is a path of bounded curvature from ω_S to ω_T.

If $I = S$, the orientation of $\mathcal{P}$ at I can only be $\vec{U}_S$ or $-\vec{U}_S$ since I is the last intersection point between $\mathcal{P}$ and $C_L(S) \cup C_R(S)$. But only the latter cases can occur since otherwise, $\mathcal{P}$ would not be optimal. As by definition, I lies before I' along $\mathcal{P}$, the part of $\mathcal{P}$ from $(S, \vec{U}_S)$ to I' is longer than the shortest Dubins path from $(S, \vec{U}_S)$ to $(S, -\vec{U}_S)$ which is a path of type CCC of length $2\pi + \pi/3$. Let SI' be the concatenation of the arc SA of $C_L(S)$ and the circular arc AI', and let $\mathcal{P}'$ be the concatenation of SI' and the part of $\mathcal{P}$ from I' to T. As, the length of SI' is at most 2π, $\mathcal{P}'$ is shorter than $\mathcal{P}$. We then get a contradiction as above.

Similar arguments hold if $\mathcal{P}$ intersects the interior of $\mathcal{R}_T$. □

Theorem 2 *If $\mathcal{R}_S$ and $\mathcal{R}_T$ are disjoint and do not intersect Ω, $\mathcal{P}$ is the Euclidean shortest path from S to T avoiding Ω and the two additional obstacles $\mathcal{R}_S$ and $\mathcal{R}_T$.*

Proof: It follows from Lemma 1 that $\mathcal{P}$ is also the shortest path from ω_S to ω_T if we consider $\mathcal{R}_S$ and $\mathcal{R}_T$ as some other (moderate) obstacles. On the other hand, the Euclidean shortest path from S to T that avoids Ω, $\mathcal{R}_S$ and $\mathcal{R}_T$ is a path of bounded curvature from $(S, \vec{U}_S)$ to $(T, \vec{U}_T)$. Hence, $\mathcal{P}$ is the Euclidean shortest path from S to T in the presence of the obstacles Ω, $\mathcal{R}_S$ and $\mathcal{R}_T$. □

Corollary 3 *A Dubins path of type CCC between two configurations ω_S and ω_T is optimal only if the two regions $\mathcal{R}_S$ and $\mathcal{R}_T$ intersect.*

In the rest of the paper, we will assume that Theorem 2 does not apply.

3 Characterization of the C-segments

We first recall the following lemma mentioned in the introduction which follows from [10] or [5] :

Lemma 4 *Each subpath of an optimal path which has no point in common with the obstacles except possibly its two end points must be of type CCC or CSC.*

We now recall three lemmas and a theorem established by Agarwal et al. [1]. For completeness, we give the proofs (in our more restricted case of moderate obstacles).

Lemma 5 *Any non-terminal C-segment of an optimal path is longer than π.*

Proof: Because the obstacles are moderate, no obstacle can touch the inner side of the C-segment. Moreover, since the C-segment is preceded and followed by some arcs, the path can be shortened using a circular arc of radius greater than 1 (see Figure 2a). □

Lemma 6 *Any optimal path does not contain a subpath of type CCC, except when the first or the last C-segments of this subpath is terminal.*

Proof: Assume for a contradiction that none of the C segments is terminal. By Lemma 5, the length of each C-segment is greater than π. Therefore, the middle C-segment together with some portions of the other two C-segments can be replaced by a shortcut which cannot be obstructed by any moderate obstacle (see Figure 3). This contradicts the hypothesis and proves that one of the C-segments is terminal. □

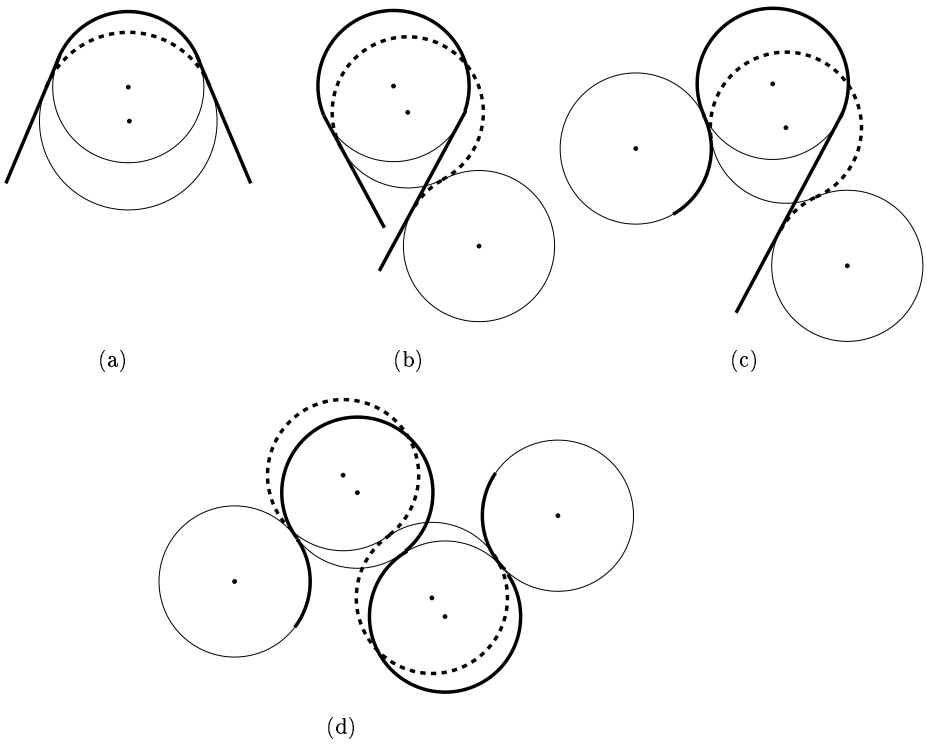

Figure 2: Dubins length-reducing perturbations

Lemma 7 *If an optimal path contains a subpath of type SCS, OCS, SCO or OCO, the C-segment is anchored.*

Proof: By Lemma 5, the C-segment is longer than π. If the C-segment is not anchored, then, according to Dubins [10], perturbations (b) and (c) of Figure 2 shorten the paths in an obstacle-free scene. That yields the lemma since the O-segments are either line segments or circular arcs of unit radius. □

Theorem 8 *Any C-segment appearing in an optimal path belongs to one of the following subpaths :*

$$\bar{\bar{C}}, \quad \bar{C}\bar{C}, \quad C_t C\bar{C}, \quad \bar{C}CC_t.$$

Proof: A C-segment either is terminal or belongs to a subpath of one of the three types XCY, $XCCY$ or CCC where $X, Y \in \{S, O\}$. If the subpath is of type XCY,

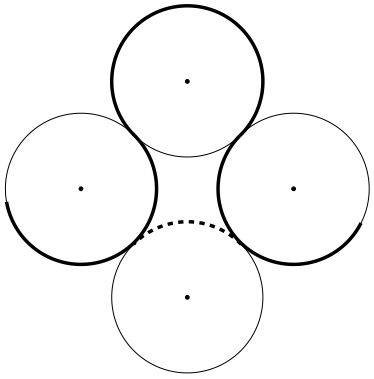

Figure 3: Shortcut of a subpath of type CCC (Lemma 6)

the C-segment is anchored by Lemma 7. If the subpath is of type $XCCY$, both C-segments must be tangent to some obstacle, due to Lemma 4. If the subpath is of type CCC, then, by Lemma 6, the first or the third C-segment must be terminal. Let us assume without loss of generality that the subpath is C_tCC. If the next segment is a C segment, it is terminal by Lemma 6 and one of the two intermediate C-segments must touch an obstacle by Lemma 4. If the next segment is not a C segment, the last C-segment must touch an obstacle by Lemma 4. □

We further restrict the possible types of C-segments that may appear in an optimal path :

Theorem 9 *Any C-segment of an optimal path belongs to one of the following subpaths :*

$$\bar{\bar{C}}, \quad \bar{C}\bar{C}, \quad C_tC\bar{\bar{C}}, \quad \bar{\bar{C}}CC_t.$$

Proof: It suffices to consider subpaths of types $C_tC\bar{C}$ or $\bar{C}CC_t$ where the $\bar{C}$-segment is not terminal. Without loss of generality, we consider subpaths of types $C_tC\bar{C}$.

Consider first an optimal subpath of type $C_tC\bar{C}O$ where the O-segment is a circular arc. We use the same perturbation that Dubins used to reduce the length of $CCCC$-paths (see Figure 2d). It follows that the second or the third C-segments of $C_tC\bar{C}O$ must be clamped by some obstacles. Hence, either the third C-segment is anchored or both the second and the third C-segments are tangent to some obstacles.

Consider now an optimal subpath of type $C_tC\bar{C}S$ and the two types of perturbation shown in Figure 4. Dubins has shown that perturbation (a) shortens the path and, as shown below, perturbation (b) also shortens the path. Thus, either the third

C-segment is anchored or both the second and the third C-segments are tangent to some obstacles.

An optimal subpath of type $C_tC\bar{C}C$ is necessarily of type $C_tC\bar{C}C_t$, in which case the third C-segment is anchored by definition.

We conclude that a subpath of type C_tCC is either of type $C_tC\bar{\bar{C}}$ or $C_t\bar{C}\bar{C}$.

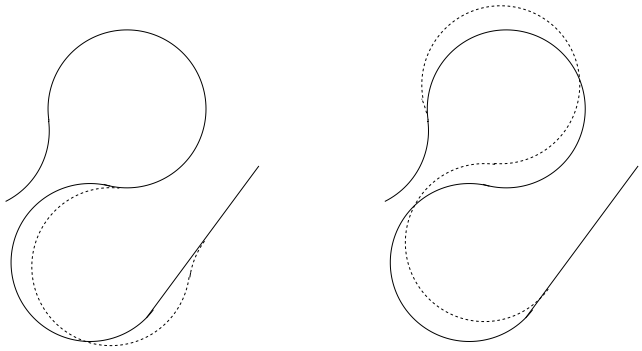

Figure 4: Length reducing perturbations for $CCCS$ paths

Now, we show that perturbation (b) of Figure 4 shortens the path of type $CCCS$. We consider, without loss of generality, that the straight line segment belongs to the x-axis and that the center of the circle supporting the first C-segment belongs to the y-axis (see Figure 5).

With the notations of Figure 5, the length of a $CCCS$ path is equal to $L = 2(u_1 + u_2) - \gamma + d - x$ where γ and d are some constants. Furthermore, we have :

$$\begin{cases} \sin(u_1) + \sin(u_2) = x/2 \\ \cos(u_1) - \cos(u_2) = (h-1)/2 \end{cases}$$

We compute the derivative of each equation with respect to x and solve the system. We obtain the following solution ($(u_1 + u_2) \in (\pi, 2\pi)$ by Lemma 5) :

$$\begin{cases} \dfrac{\partial u_1}{\partial x} = \dfrac{\sin(u_2)}{2\sin(u_1+u_2)} \\ \dfrac{\partial u_2}{\partial x} = \dfrac{\sin(u_1)}{2\sin(u_1+u_2)} \end{cases}$$

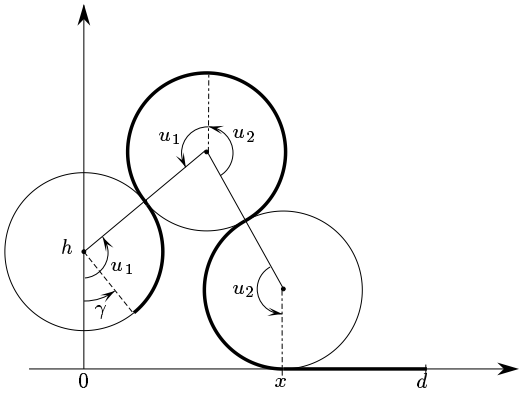

Figure 5: Study of the perturbation (b) of Figure 4

Therefore,

$$\frac{\partial L}{\partial x} = \frac{\sin(u_1) + \sin(u_2)}{\sin(u_1 + u_2)} - 1 = \frac{\cos\left(\frac{u_1 - u_2}{2}\right) - \cos\left(\frac{u_1 + u_2}{2}\right)}{\cos\left(\frac{u_1 + u_2}{2}\right)},$$

which is negative since u_1 and u_2 are positive and $(u_1 + u_2) \in (\pi, 2\pi)$. Hence, perturbation (b) of Figure 4 shortens a path of type $CCCS$. □

As, for a given set of obstacles, the number of anchored circles is finite, the number of the subpaths in Theorem 9 is finite except for the subpaths of type $\bar{C}\bar{C}$. The two following sections will show that the number of these subpaths is also finite. First, in Section 4, we will show that any non-terminal subpath of type $\bar{C}\bar{C}$ of an optimal path is necessarily contained in a subpath of type $XS\bar{C}\bar{C}SX'$ where $X, X' \in \{O, \bar{\bar{C}}\}$. Then, in Section 5, we will show that, given X, X' and two obstacle edges, the number of subpaths of an optimal path of type $XS\bar{C}\bar{C}SX'$ where the C-segments are tangent to the given obstacle edges is finite.

4 Characterization of the subpaths of type $\bar{C}\bar{C}$

The section is devoted to the proof of the following theorem :

Theorem 10 *Any non terminal subpath of type $\bar{C}\bar{C}$ of an optimal path is necessarily contained in a subpath of type $XS\bar{C}\bar{C}SX'$ where $X, X' \in \{O, \bar{\bar{C}}\}$. The length of S-segment may be zero.*

In the sequel, we will use the following notations. For a given subpath $\mathcal{P}$, C_i will denote the i-th C-segment of $\mathcal{P}$, $\mathcal{C}_i$ will denote the circle supporting C_i and O_i the center of $\mathcal{C}_i$ ($i \in \{1, 2, 3\}$).

We first establish two lemmas and a proposition.

Lemma 11 *In a subpath of type CCS of an optimal path where the first C-segment is not terminal, the length of the S-segment is smaller than $4\cos\alpha$. Here $\alpha = \angle(\overrightarrow{O_2O_1}, \vec{u})$ and $\vec{u}$ is the direction of the S-segment (see Figure 6).*

Proof: Let $\mathcal{P}$ be the optimal subpath of type CCS. Since the length of each C-segment is strictly greater than π and smaller than 2π, α belongs to $(-\pi/2, \pi/2)$ (see Figure 6). We distinguish three cases according to the value of α and, in each case, we exhibit a shortcut that clearly cannot intersect the moderate obstacles.

1. $\alpha \in (0, \pi/2)$ (Figure 6a) : if the length of the S-segment is greater than $4\cos\alpha$, the dashed C-segment shortens $\mathcal{P}$.

2. $\alpha \in (-\pi/2, -\pi/3)$ (Figure 6b) : let $\mathcal{C}'$ be the circle (of unit radius) tangent to $\mathcal{C}_1$ and to the S-segment,and lying on the same side of S as $\mathcal{C}_2$. As $|\alpha| > \pi/3$, $\mathcal{C}'$ intersects $\mathcal{C}_2$ and therefore the length of the dashed C-segment on $\mathcal{C}_1$ is smaller than $\pi/3$. Moreover, the length of the dashed C-segment on $\mathcal{C}'$ is smaller than $\pi/2$ because the line segment intersects $\mathcal{C}_1$. It follows that the length of the dashed path is smaller than π and so is smaller than the length of the C-segment supported by $\mathcal{C}_2$. Hence, if the length of the S-segment is greater than $4\cos\alpha$, the dashed path shortens $\mathcal{P}$.

3. $\alpha \in [-\pi/3, 0]$ (Figures 6c and 6d) : if the length of the S-segment is greater than 2 ($\leq 4\cos\alpha$), then the path that uses the dashed arcs AB and CD is shorter than $\mathcal{P}$. Indeed, the length of the dashed C-segment AB is shorter than the sum of the lengths of the arcs AI and IB of $\mathcal{P}$, and similarly the length of the dashed C-segment CD is shorter than sum of the lengths of the arcs CI and ID.

□

We consider now subpaths of type $CCSC$.

Lemma 12 *Let $\mathcal{P}$ be a subpath of type $CCSC$ of an optimal path where the first and the last C-segments are not terminal. If the two C-segments C_2 and C_3 that are adjacent to the line segment have the same orientation (resp. the opposite orientation), the distance between O_1 and O_3 is less than 2 (resp. 4).*

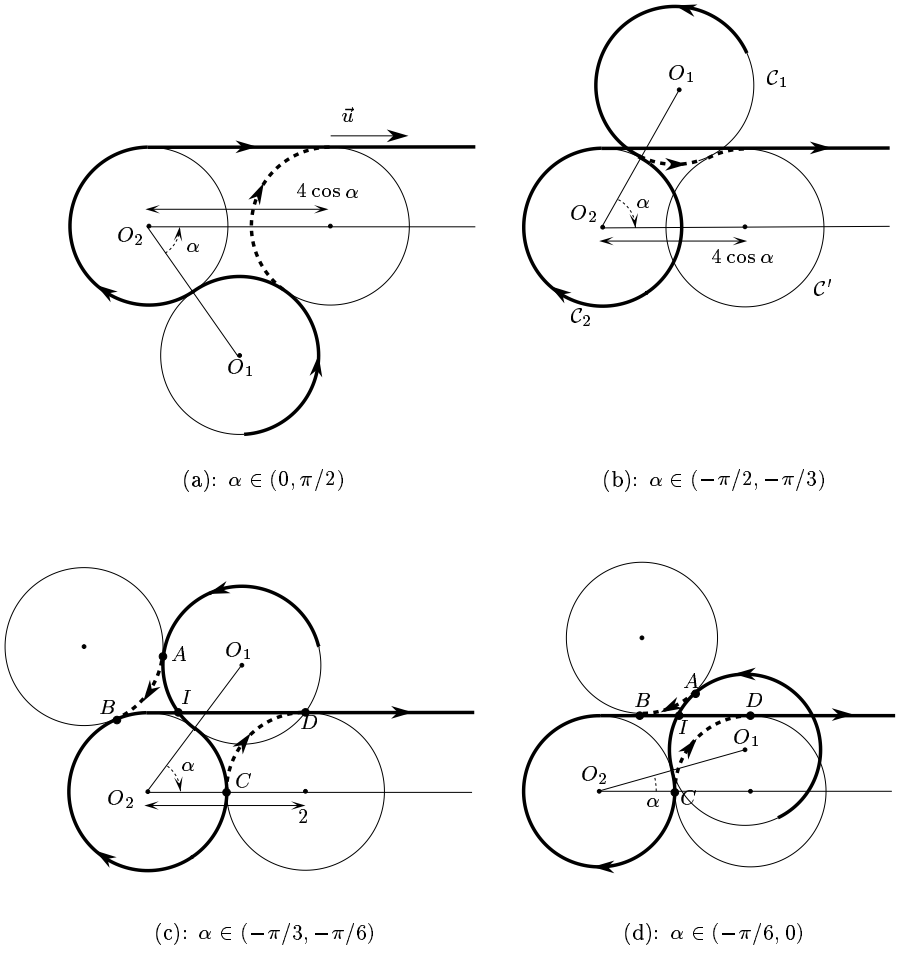

(a): $\alpha \in (0, \pi/2)$ (b): $\alpha \in (-\pi/2, -\pi/3)$

(c): $\alpha \in (-\pi/3, -\pi/6)$ (d): $\alpha \in (-\pi/6, 0)$

Figure 6: Shortcuts used in Lemma 11

Proof: By the previous lemma, the length s of the S-segment is less than $4\cos\alpha$.

If $\mathcal{C}_2$ and $\mathcal{C}_3$ have the same orientation,

$$O_1O_3^2 = (\overrightarrow{O_1O_2} + \overrightarrow{O_2O_3})^2 = 4 + s^2 - 4s\cos\alpha < 4.$$

If the two circles have opposite orientations, let O_3' be the point symmetric to O_3 with respect to the S-segment. The length of O_1O_3 is less than the sum of the

length of O_3O_3', which is equal to 2, and of the length of O_1O_3', which is less than 2 by the above inequality. □

Lemma 13 *In a subpath of type $CCSC$ of an optimal path where the first and the last C-segments are not terminal, the two C-segments adjacent to the line segment have the same orientation (clockwise or counterclockwise).*

Proof: We consider a subpath $\mathcal{P}$ of type $CCSC$ of an optimal path where C_1 and C_3 are not terminal and such that C_2 and C_3 have opposite orientations. We show that such a path can be shortened. The previous lemma implies that there exists a circle of unit radius tangent to the circles $\mathcal{C}_1$ and $\mathcal{C}_3$.

Suppose first that the circles $\mathcal{C}_1$ and $\mathcal{C}_3$ do not intersect. Since the length of C_1 and C_3 are greater than π, there exists a C-segment of length smaller than π tangent to both C_1 and C_3 (see Figure 7). This C-segment clearly shortens $\mathcal{P}$ and avoids the moderate obstacles.

Suppose now that $\mathcal{C}_1$ and $\mathcal{C}_3$ intersect. The previous argument does not hold since there does not necessarily exists a circle tangent to the C-segments C_1 and C_3 (see Figure 8a). However, the shortcut shown in Figure 8 shortens $\mathcal{P}$ since the length of the dashed C-segment AB is shorter than the sum of the lengths of the arcs AI and IB of $\mathcal{P}$, and, similarly, the length of the dashed C-segment CD is shorter than the sum of the lengths of the arcs CI and ID. □

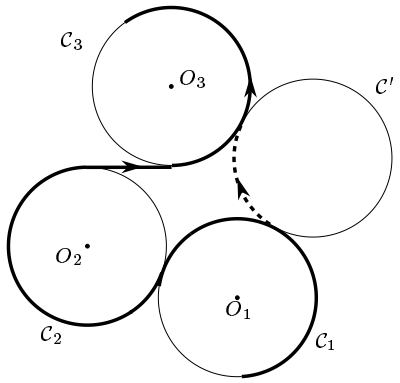

Figure 7: Shortcut used in Lemma 13 if $\mathcal{C}_1$ does not intersect $\mathcal{C}_3$

Proposition 14 *An optimal path cannot contain a subpath of type $CCSCC$, except when the first or the last C-segment of this subpath is terminal.*

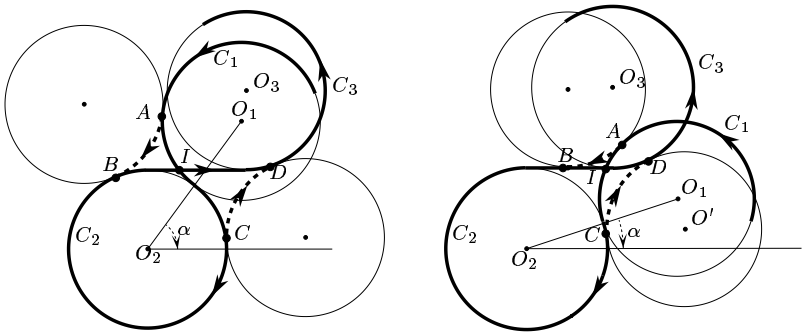

(a): $\alpha \in (-\pi/2, -\pi/6)$ (b): $\alpha \in (-\pi/6, 0)$

Figure 8: Shortcut used in Lemma 13 if $\mathcal{C}_1$ does intersect $\mathcal{C}_3$

Proof: By Lemma 5, the lengths of C_1 and C_4 are greater than π if they are not terminal. According to the previous lemma, both C-segments C_2 and C_3 have the same orientation. We assume, without loss of generality, that the first C-segment C_1 is oriented counterclockwise. Then, we show that the dashed C-segment shown in Figure 9 shortens the path. Let M_{12} be the common end point of C_1 and C_2, and M_{34} the common end point of C_3 and C_4 (see Figure 9). Let α and β be defined as in Figure 9 and let s be the length of the S-segment.

We show now that there exists a C-segment of length smaller than π oriented clockwise and tangent to C_1 and C_4. By Lemma 12, the length of O_2O_4 is less than 2, implying that the length of O_1O_4 is less than 4. Thus there exist two circles of unit radius tangent to $\mathcal{C}_1$ and $\mathcal{C}_4$. As the length of O_2O_4 is less than 2, M_{12} belongs to the dashed C-segment between A and B on Figure 10. As C_1 is oriented counterclockwise and its length is greater than π, point B belongs to C_1 (see Figure 10). Similarly, point D belongs to C_4. Moreover, the C-segment oriented clockwise and tangent to $\mathcal{C}_1$ at B and to $\mathcal{C}_4$ at D is smaller than π. It follows that this C-segment shortens the subpath of type $CCSCC$. As it avoids all the moderate obstacles, we have shown that an optimal path can not contain a subpath of type $CCSCC$ except when the first or the last C-segment of this subpath is terminal. □

The proof of Theorem 10 now follows. Indeed, let us consider a subpath of type $XS\bar{C}\bar{C}SX'$, $X \notin \{O, \bar{\bar{C}}\}$. As X is not terminal, Lemma 6 implies that the first S-segment of the subpath cannot have length zero. Therefore, by Theorem 9, X is necessarily a C-segment tangent to some obstacle and following another C-segment X_1.

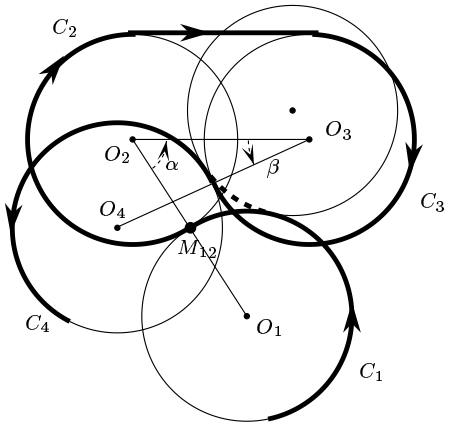

Figure 9: Shortcut used in Proposition 14

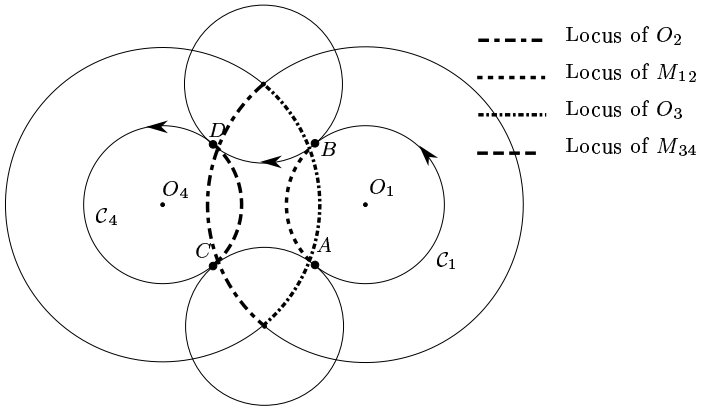

Figure 10: For the proof of Proposition 14

Then, by Proposition 14, X_1 is terminal and therefore, X is anchored by definition. This contradicts our assumption and ends the proof of the theorem.

5 Bounding the number of subpaths of type $\bar{C}\bar{C}$

This section is devoted to the proof of the following theorem :

Theorem 15 *Let $\mathcal{X}$ (resp. $\mathcal{X}'$) be a circular edge of some obstacle or an anchored circle, and let $\mathcal{O}$ and $\mathcal{O}'$ be two obstacle edges. Let $X \subset \mathcal{X}$, $X' \subset \mathcal{X}'$, $\bar{C}$ a C-segment tangent to $\mathcal{O}$ and $\bar{C}'$ a C-segment tangent to $\mathcal{O}'$. The shortest subpath of type $XS\bar{C}\bar{C}'SX'$ belong to a finite family.*

Let $\mathcal{P}$ denote a subpath of type $XS\bar{C}\bar{C}'SX'$. The number of subpaths $\mathcal{P}$ where $\bar{C}$ or $\bar{C}'$ are anchored is finite; so we assume that neither $\bar{C}$ nor $\bar{C}'$ are anchored. Without loss of generality, we assume in the sequel that the path $\mathcal{P}$ is oriented counterclockwise on $\bar{C}$ and clockwise on $\bar{C}'$ as shown in Figures 11, 15 and 17.

The proof is as follows. We first observe that $\mathcal{P}$ is optimal when some mechanical device is at equilibrium. This leads to an algebraic system of equations whose solutions correspond to potential equilibriums of the mechanical device. We then show that this system has a finite number of solutions. This is done as follows. Let $E_1 = 0, \ldots, E_r = 0$ be the equations of the system where $E_1, \ldots, E_r$ are polynomials in the variables $x_1, \ldots, x_r$. The resultant $R(x_1, \ldots, x_{r-1})$ with respect to x_r of two of the E_i, say E_1 and E_2, vanishes at $\tilde{x}_1, \ldots, \tilde{x}_{r-1}$ iff there exists $\tilde{x_r}$ such that $(\tilde{x}_1, \ldots, \tilde{x}_{r-1}, \tilde{x}_r)$ is a common root of E_1 and E_2 [3]. By cascading resultants on the polynomials $E_1, \ldots, E_r$, we eliminate successively the indeterminates $x_r, \ldots, x_2$ and compute a univariate polynomial $R(x_1)$. If $(\tilde{x}_1, \ldots, \tilde{x}_r)$ is a solution of the system, $R(\tilde{x}_1) = 0$ (the converse is not necessarily true). Then we show that the univariate polynomial $R(x_1)$ is not identically zero and that any value of the indeterminate x_1 determines the other indeterminates. It immediately follows that the algebraic system of equations under consideration has a finite number of roots. However, computing such a polynomial $R(x_1)$ may exceed the capabilities of the current computer algebra systems. To overcome this difficulty, we only compute the leading monomial of $R(x_1)$ which is sufficient to show that $R(x_1) \not\equiv 0$. We now present the proof in full detail.

The mechanical device consists of four fixed objects and one moving object D. The fixed objects are the two obstacles $\mathcal{O}$ and $\mathcal{O}'$ and the two disks of unit radius supporting $\mathcal{X}$ and $\mathcal{X}'$. The moving object D is the union of two tangent disks (corresponding to the circles $\mathcal{C}$ and $\mathcal{C}'$). We consider a rubber band of thickness zero attached on $\mathcal{X}$ and on $\mathcal{X}'$ and passing around $\mathcal{C}$ and $\mathcal{C}'$ (see Figure 11). The case we are interested in is when both mobile disks are tangent to the obstacles. The moving object D is subject to four forces $\overrightarrow{F}$, $\overrightarrow{F'}$, $\overrightarrow{R}$ and $\overrightarrow{R'}$ (see Figure 11). $\overrightarrow{F}$ and $\overrightarrow{F'}$ are the two forces, of equal norm F, exerted by the rubber band. $\overrightarrow{R}$ and $\overrightarrow{R'}$ are the reactions of the obstacles $\mathcal{O}$ and $\mathcal{O}'$ onto the mobile D.

We introduce the following notations (see Figures 11 and 12). Let $\mathcal{C}$ and $\mathcal{C}'$ be the circles supporting $\bar{C}$ and $\bar{C}'$. I and I' are the centers of $\mathcal{C}$ and $\mathcal{C}'$. H and H'

are the centers of the circles supporting $\mathcal{X}$ and $\mathcal{X}'$. In addition, let $\alpha = \angle(\overrightarrow{R}, \overrightarrow{II'})$, $\alpha' = \angle(\overrightarrow{R'}, \overrightarrow{I'I})$, $\varphi = \angle(\overrightarrow{II'}, \overrightarrow{F})$ and $\varphi' = \angle(\overrightarrow{I'I}, \overrightarrow{F'})$.

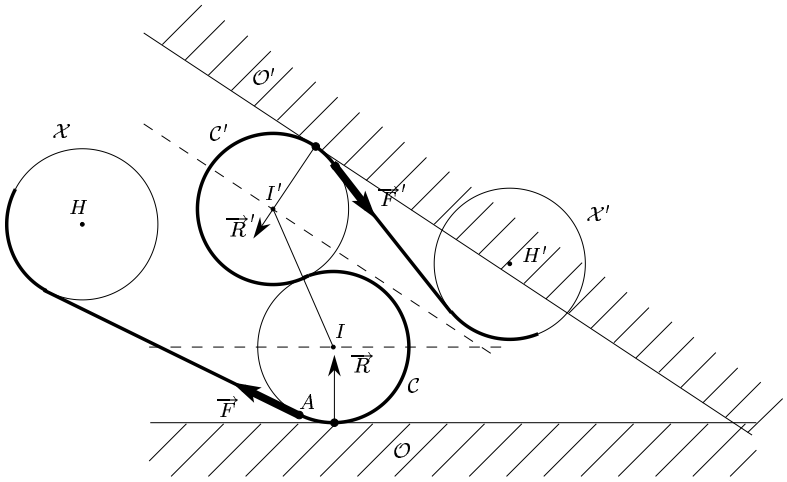

Figure 11: The mechanical device

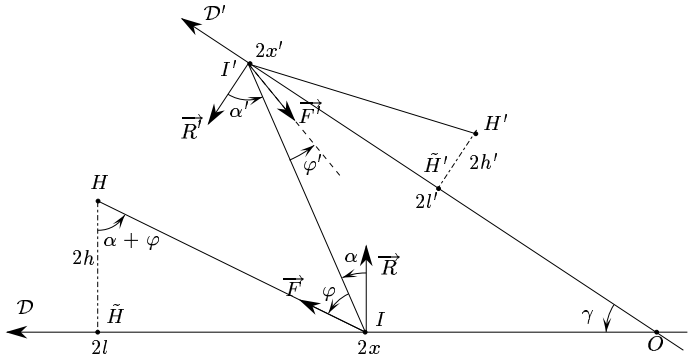

Figure 12: For the proof of Theorem 15

We first establish a lemma that holds regardless of the nature of the obstacle edges $\mathcal{O}$ and $\mathcal{O}'$.

Lemma 16 *The moving object D is at an equilibrium only if :*

$$\sin(\alpha' - \alpha) + \sin\alpha' \sin(\alpha + \varphi) - \sin\alpha \sin(\alpha' + \varphi') = 0 \quad (1)$$

Proof: The moving object D is at an equilibrium iff the sum of the forces $\overrightarrow{F}$, $\overrightarrow{F'}$, $\overrightarrow{R}$, $\overrightarrow{R'}$ and the sum of their torques is zero. The sum of the forces is zero iff :

$$\begin{cases} R\cos\alpha + F\cos\varphi = R'\cos\alpha' + F\cos\varphi' \\ R\sin\alpha - F\sin\varphi = R'\sin\alpha' - F\sin\varphi' = F \end{cases}$$

We consider the torque of the forces with respect to I'; let A be the supporting point of the force $\overrightarrow{F}$ on $\mathcal{C}$:

$$\begin{aligned} \mathcal{M}_{\overrightarrow{F}/I'} &= \overrightarrow{F} \times \overrightarrow{AI'} = \overrightarrow{F} \times \overrightarrow{AI} + \overrightarrow{F} \times \overrightarrow{II'} \\ &= -F - 2F\sin\varphi \\ \mathcal{M}_{\overrightarrow{F'}/I'} &= -F \\ \mathcal{M}_{\overrightarrow{R}/I'} &= 2R\sin\alpha \\ \mathcal{M}_{\overrightarrow{R'}/I'} &= 0 \end{aligned}$$

The sum of these torques is zero iff $R\sin\alpha - F\sin\varphi = F$. Thus the moving object D is at an equilibrium iff :

$$\begin{cases} R\cos\alpha + F\cos\varphi = R'\cos\alpha' + F\cos\varphi' \\ R\sin\alpha - F\sin\varphi = R'\sin\alpha' - F\sin\varphi' \end{cases}$$

By eliminating R and R', we get :

$$\begin{aligned} &(F + F\sin\varphi)\cos\alpha\sin\alpha' + F\cos\varphi\sin\alpha\sin\alpha' = \\ &\quad (F + F\sin\varphi')\cos\alpha'\sin\alpha + F\cos\varphi'\sin\alpha\sin\alpha' \end{aligned}$$

Equation 1 follows. □

Case 1 : Both obstacle edges are line segments

Let $\mathcal{D}$ (resp. $\mathcal{D}'$) be the oriented line parallel to $\mathcal{O}$ ($\mathcal{O}'$), passing through I (I') and oriented such that $\angle(\overrightarrow{R}, \mathcal{D}) = \pi/2$ ($\angle(\overrightarrow{R'}, \mathcal{D}') = -\pi/2$) (see Figure 12).

Let $\gamma = \angle(\mathcal{D}', \mathcal{D})$. Let O be the intersection point between $\mathcal{D}$ and $\mathcal{D}'$ (O is well defined since no two obstacle edges are parallel). Let $\tilde{H}$ ($\tilde{H}'$) be the orthogonal

projection of H (H') onto $\mathcal{D}$ ($\mathcal{D}'$). Let $2x$ and $2l$ (resp. $2x'$, $2l'$) be the algebraic lengths of OI and $O\tilde{H}$ (OI', $O\tilde{H}'$) on the oriented line $\mathcal{D}$ ($\mathcal{D}'$). Let $2h$ be the algebraic distance between H and $\mathcal{D}$ with $2h > 0$ iff $\overrightarrow{\tilde{H}H}$ and $\overrightarrow{R}$ have the same orientation; $2h'$ is defined similarly except that $2h' > 0$ iff $\overrightarrow{\tilde{H}'H'}$ and $\overrightarrow{R'}$ have opposite orientations.

Lemma 17 *The moving object D is at an equilibrium only if :*

$$\begin{cases} \sin\gamma + \sin(\alpha+\gamma)\sin(\alpha+\varphi) - \sin\alpha\sin(\alpha'+\varphi') = 0 \\ h\sin\gamma\sin(\alpha+\varphi) - l\sin\gamma\cos(\alpha+\varphi) + \cos(\alpha+\gamma)\cos(\alpha+\varphi) + \delta\sin\gamma = 0 \\ h'\sin\gamma\sin(\alpha'+\varphi') - l'\sin\gamma\cos(\alpha'+\varphi') + \cos\alpha\cos(\alpha'+\varphi') + \delta'\sin\gamma = 0 \end{cases} \quad (2)$$

where δ (resp. δ') is zero if the path $\mathcal{P}$ has the same orientation on $\mathcal{X}$ and $\mathcal{C}$ ($\mathcal{X}'$ and $\mathcal{C}'$) and 1 otherwise.

Proof: Considering the triangle (OII') in Figure 12 yields :

$$\alpha' = \alpha + \gamma \ [2\pi] \quad (3)$$

$$\frac{|\sin\gamma|}{2} = \frac{|\sin(\alpha+\pi/2)|}{|2x'|} = \frac{|\sin(\pi/2-\alpha')|}{|2x|}$$

Considering the different cases that may appear, we get :

$$x = \frac{\cos\alpha'}{\sin\gamma} \qquad x' = \frac{\cos\alpha}{\sin\gamma} \quad (4)$$

Equations 1 and 3 yield the first equation of System 2. We show how to compute the two other equations of System 2 for each possible orientation of X and X'.

- $\mathcal{P}$ has the same orientation on $\mathcal{X}$ and $\mathcal{C}$.

By definition of α and φ, $\alpha+\varphi = \angle(\overrightarrow{R}, \overrightarrow{F})\ [2\pi] = \angle(\overrightarrow{HH}, \overrightarrow{HI})\ [\pi]$. As $\overrightarrow{HH}$ and $\overrightarrow{\tilde{H}I}$ are orthogonal, $\tan(\alpha+\varphi) = \pm(2l-2x)/2h$ (see Figure 12). Considering the different cases that may appear (see Table 1 and Figure 12), we get :

$$\tan(\alpha+\varphi) = \frac{l-x}{h} \quad (5)$$

Using Equations 3 and 4, we obtain :

$$h\sin\gamma\sin(\alpha+\varphi) - l\sin\gamma\cos(\alpha+\varphi) + \cos(\alpha+\gamma)\cos(\alpha+\varphi) = 0 \quad (6)$$

- $\mathcal{P}$ has the same orientation on $\mathcal{X}'$ and $\mathcal{C}'$.

$\alpha+\varphi$	$-\pi$	$-\pi/2$	0	$\pi/2$	π
$\tan(\alpha+\varphi)$	+	−	+	−	
$l-x$	−	−	+	+	
h	−	+	+	−	

Table 1: Respective signs of $\tan(\alpha+\varphi)$, $l-x$ and h.

Similarly as above, we obtain :

$$\tan(\alpha'+\varphi') = \frac{l'-x'}{h'} \tag{7}$$

$$h'\sin\gamma\sin(\alpha'+\varphi') - l'\sin\gamma\cos(\alpha'+\varphi') + \cos\alpha\cos(\alpha'+\varphi') = 0 \tag{8}$$

• $\mathcal{P}$ has opposite orientations on $\mathcal{X}$ and $\mathcal{C}$.

Let $\mu = \angle(\overrightarrow{F}, \overrightarrow{IH})$ and $\varepsilon = \angle(\overrightarrow{IH}, \mathcal{D})$ (see Figure 13). With these definitions, we have :

$$\alpha+\varphi+\mu+\varepsilon = \pi/2 \ [2\pi]$$

$$\sin\mu = \frac{2}{IH} \quad \sin\varepsilon = \frac{2h}{IH} \quad \cos\varepsilon = \frac{2l-2x}{IH}$$

Therefore, $\alpha+\varphi+\varepsilon = \pi/2-\mu \ [2\pi]$, $\cos(\alpha+\varphi)\cos\varepsilon - \sin(\alpha+\varphi)\sin\varepsilon = \sin\mu$, and :

$$(l-x)\cos(\alpha+\varphi) - h\sin(\alpha+\varphi) = 1 \tag{9}$$

By Equations 3 and 4, we obtain :

$$h\sin\gamma\sin(\alpha+\varphi) - l\sin\gamma\cos(\alpha+\varphi) + \cos(\alpha+\gamma)\cos(\alpha+\varphi) + \sin\gamma = 0 \tag{10}$$

• $\mathcal{P}$ have opposite orientations on $\mathcal{X}'$ and $\mathcal{C}'$.

Let $\mu' = \angle(\overrightarrow{F'}, \overrightarrow{I'H'})$ and $\varepsilon' = \angle(\overrightarrow{I'H'}, \mathcal{D}')$ (see Figure 14). We have :

$$\alpha'+\varphi'+\mu'+\varepsilon' = -\pi/2 \ [2\pi]$$

$$\sin\mu' = \frac{2}{I'H'} \quad \sin\varepsilon' = -\frac{2h'}{I'H'} \quad \cos\varepsilon' = \frac{2x'-2l'}{I'H'}$$

Therefore, $\alpha'+\varphi'+\varepsilon' = -\pi/2-\mu'$, $\cos(\alpha'+\varphi')\cos\varepsilon' - \sin(\alpha'+\varphi')\sin\varepsilon' = -\sin\mu'$, and :

$$(x'-l')\cos(\alpha'+\varphi') + h'\sin(\alpha'+\varphi') = -1 \tag{11}$$

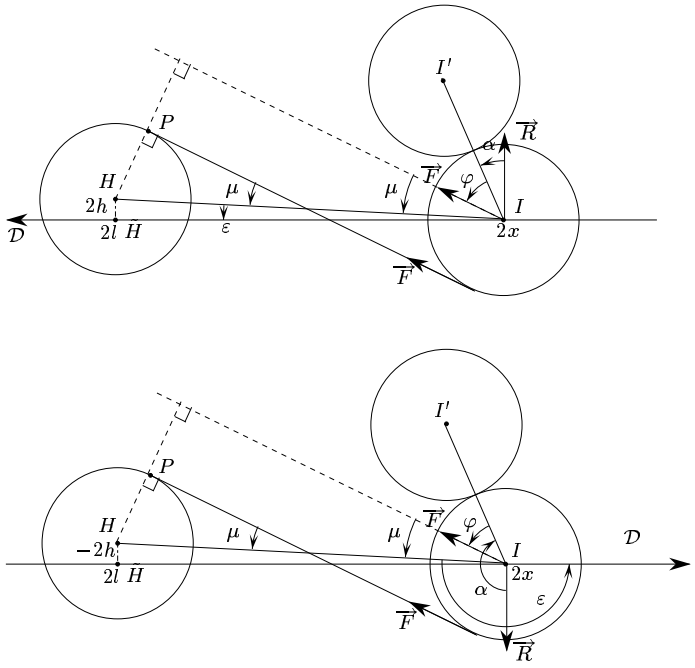

Figure 13: Computing Equations 10

Then, by Equation 4 :

$$h' \sin\gamma \sin(\alpha' + \varphi') - l' \sin\gamma \cos(\alpha' + \varphi') + \cos\alpha \cos(\alpha' + \varphi') + \sin\gamma = 0 \qquad (12)$$

That ends the proof of the lemma. □

We consider System 2 as a system of three equations in the three indeterminates α, $(\alpha + \varphi)$, $(\alpha' + \varphi')$ and show that it has a finite number of roots in $(S^1)^3$. It then follows that the moving object D has a finite number of equilibriums because α determines α' by Equation 3.

Using the variable substitution $x = \tan(\frac{\alpha}{2})$, $y = \tan(\frac{\alpha+\varphi}{2})$ and $z = \tan(\frac{\alpha'+\varphi'}{2})$, we transform System 2 into an algebraic system where x, y, z are the indeterminates and h, l, h', l', $\sin\gamma$, $\cos\gamma$ are considered as six independent parameters. Let $E_i = 0$ ($i \in \{1, 2, 3\}$) denote the algebraic equation obtained from the i-th equation of System 2.

Using MAPLE, we compute the resultant $Q(x, z)$ of E_1 and E_2 with respect to the indeterminate y. Then, we compute the resultant $R(x)$ of $Q(x, z)$ and E_3 with

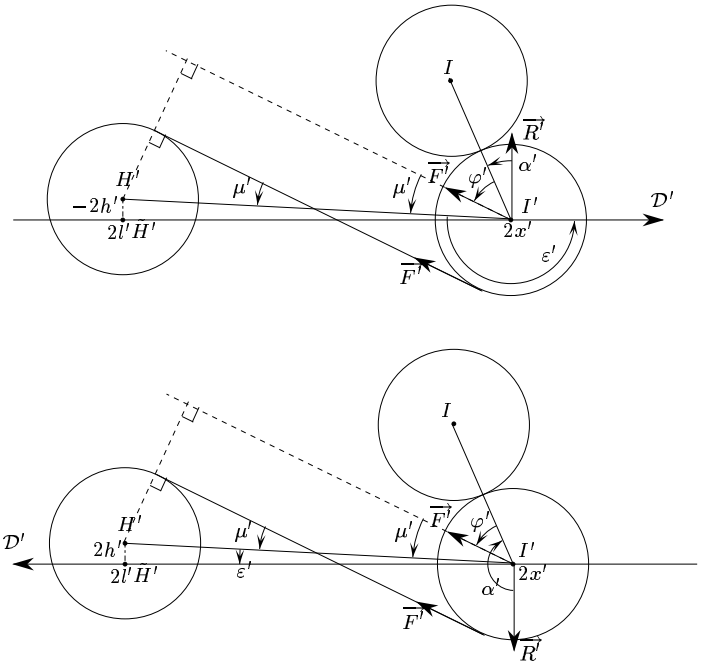

Figure 14: Computing Equations 12

respect to the indeterminate z. $R(x)$ is a uni-variate polynomial of degree 24. Any root of System 2 verifies $R(\tan(\alpha/2)) = 0$. Moreover, if x is given, then α, α', φ and φ' are fixed (see Figure 12), and so y and z are fixed. Therefore, if $R(x) \not\equiv 0$, the mechanical device admits a finite number of equilibriums.

We now prove that $R(x) \not\equiv 0$. The leading and the trailing monomials of $R(x)$ are

$$2^8\,(h+\delta)^4 \sin^8\gamma\,((1+l'\sin\gamma)^2 + h'^2\sin^2\gamma)^2\,x^{24},$$
$$2^8\,(h-\delta)^4 \sin^8\gamma\,((1-l'\sin\gamma)^2 + h'^2\sin^2\gamma)^2.$$

Both coefficients are zero only if $h = \delta = 0$ or if (h, h', l') is equal to either $(1, 0, -1/\sin\gamma)$ or $(-1, 0, 1/\sin\gamma)$ because, by hypothesis, $\sin\gamma \neq 0$ and $\delta \in \{0, 1\}$. If $h = \delta = 0$ then $\cos(\alpha + \varphi) = 0$ and so $E_2 = 0$; hence, the leading and the trailing coefficients (with respect to x) of the resultant of E_1 and E_3 with respect to z are

$$4\sin^2\gamma\,(y-1)^4\,((1+l'\sin\gamma)^2 + h'^2\sin^2\gamma),$$

$$4\,\sin^2\gamma\,(y+1)^4\,((1-l'\sin\gamma)^2+h'^2\sin^2\gamma),$$

where $y = \sin(\alpha+\varphi) = \pm 1$. These two coefficients are zero only if $(h', l') = (0, \pm 1/\sin\gamma)$. Therefore, the leading and the trailing coefficients of $R(x)$ are zero only if (h, h', l') is either $(\delta, 0, -1/\sin\gamma)$ or $(-\delta, 0, 1/\sin\gamma)$. We substitute, in turn, (h, h', l') to those values in $R(x)$. When $(h, h', l') = (\delta, 0, -1/\sin\gamma)$, the leading and trailing monomials of $R(x)$ become

$$2^{12}\,\delta'^4\,\sin^4\gamma\,((l\sin\gamma+\cos\gamma)^2+\delta^2\sin^2\gamma)^2\,x^{20},$$

$$2^{14}\,\sin^4\gamma\,(\delta'^2-4)\,(l\sin\gamma-\cos\gamma)^4\,x^2,$$

and when $(h, h', l') = (-\delta, 0, 1/\sin\gamma)$, the leading and trailing monomials of $R(x)$ become

$$2^{14}\,\sin^4\gamma\,(\delta'^2-4)\,(l\sin\gamma+\cos\gamma)^4\,x^{22},$$

$$2^{12}\,\delta'^4\,\sin^4\gamma\,((l\sin\gamma-\cos\gamma)^2+\delta^2\sin^2\gamma)^2\,x^4.$$

We study the two cases $\delta' = 0$ and $\delta' = 1$: if $\delta' = 0$, $R(x) \equiv 0$ only if (h, h', l', l) is equal to either $(\delta, 0, -1/\sin\gamma, \cot\gamma)$ or $(-\delta, 0, 1/\sin\gamma, -\cot\gamma)$. For those values of (h, h', l', l) the leading or the trailing coefficient of the new resultant $R(x)$ is $2^{16}\,\delta^4\,\sin^8\gamma$. Furthermore, if $\delta = 0$, the leading or the trailing coefficient of the new resultant $R(x)$ is $-2^{20}\,\sin^8\gamma$, which is not zero. If $\delta' = 1$, $R(x) \equiv 0$ only if $\delta = 0$, $\gamma = \pm\pi/2$ and $(h, h', l', l) = (0, 0, \pm 1, 0)$. Then either the coefficient of degree 2 (if $l' = 1$) or the one of degree 4 (if $l' = -1$) of the resultant of E_1 and E_3 with respect to z is 64.

Hence, the uni-variate polynomial $R(x)$ is not identically zero, which implies that the number of possible equilibriums of our mechanical device is finite. Furthermore, they can be computed by solving $R(x) = 0$.

Case 2 : Both obstacle edges are circular arcs

The skeleton of the proof is similar to the previous case : we compute a system of 4 equations in 4 indeterminates whose solutions correspond to potential equilibriums of the mechanical device. Then, we consider a univariate polynomial $R(x)$ by cascading resultants as explained above. As computing such a polynomial $R(x)$ exceeds the capabilities of the current computer algebra systems, we only compute the leading monomial of $R(x)$ and show that it is not identically equal to zero, which implies that $R(x) \not\equiv 0$.

Let O and O' be the centers of the circles (of unit radius) supporting $\mathcal{O}$ and $\mathcal{O}'$ respectively. Let $2d$ be the length of OO'. Let $2h$ and $2h'$ be the lengths of OH and $O'H'$ respectively. Let $\omega = \angle(\overrightarrow{OO'}, \overrightarrow{OH})$ and $\omega' = \angle(\overrightarrow{O'O}, \overrightarrow{O'H'})$ (see Figure 15).

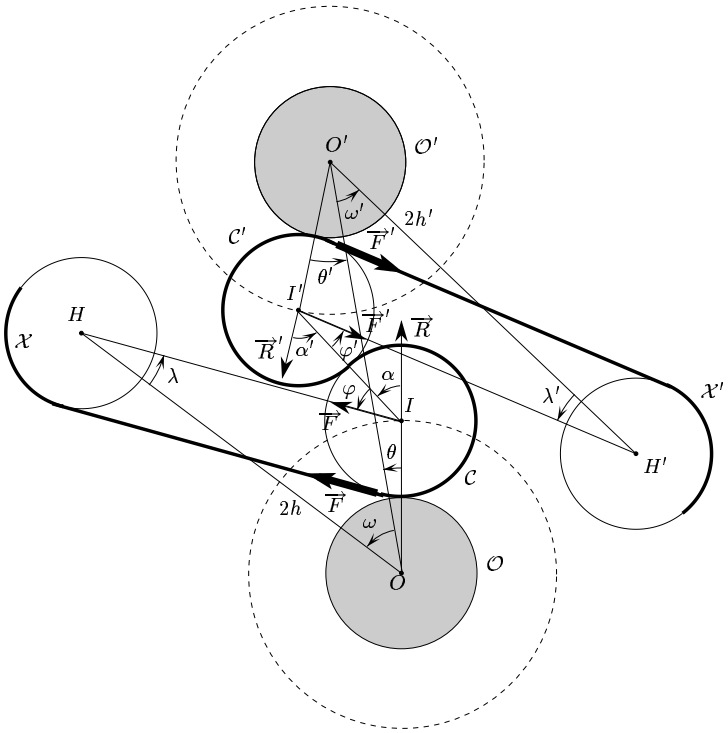

Figure 15: Mechanical device where both obstacle edges are circular edges

Lemma 18 *The moving object D is at an equilibrium only if :*

$$\begin{cases} \sin(\alpha'-\alpha)+\sin\alpha'\sin(\alpha+\varphi)-\sin\alpha\sin(\alpha'+\varphi')=0 \\ 2\cos\alpha+2\cos\alpha'+2\cos(\alpha'-\alpha)+3-d^2=0 \\ h\sin(\varphi-\omega)+h\sin(\alpha'+\varphi-\omega)+h\sin(\alpha+\varphi-\omega)-d\sin(\alpha+\varphi)+\delta d=0 \\ h'\sin(\varphi'-\omega')+h'\sin(\alpha+\varphi'-\omega')+h'\sin(\alpha'+\varphi'-\omega')-d\sin(\alpha'+\varphi')+\delta' d=0 \end{cases} \tag{13}$$

where δ (resp. δ') is zero if the path $\mathcal{P}$ has the same orientation on $\mathcal{X}$ and $\mathcal{C}$ ($\mathcal{X}'$ and $\mathcal{C}'$) and 1 otherwise.

Proof: The first equation of System 13 is given by Lemma 16. Now, let $\theta = \angle(\overrightarrow{OI}, \overrightarrow{OO'})$ and $\theta' = \angle(\overrightarrow{O'I'}, \overrightarrow{O'O})$ (see Figure 15). Considering the polygon $(OII'O')$ in Figure 15, we have :

$$\alpha' - \theta' = \alpha - \theta \ [2\pi] \tag{14}$$

$$\cos\theta + \cos(\alpha - \theta) + \cos\theta' = d \tag{15}$$
$$\sin\theta - \sin(\alpha - \theta) + \sin\theta' = 0 \tag{16}$$

Considering in turn $((Eq15)^2+(Eq16)^2)$, $((Eq15)\sin\theta-(Eq16)\cos\theta)$, $((Eq15)\cos\theta+(Eq16)\sin\theta)$, $((Eq15)\sin\theta' - (Eq16)\cos\theta')$ and
$((Eq15)\cos\theta' + (Eq16)\sin\theta')$, we obtain :

$$2\cos\alpha + 2\cos\alpha' + 2\cos(\alpha' - \alpha) + 3 - d^2 = 0 \tag{17}$$
$$d\sin\theta = \sin\alpha - \sin(\alpha' - \alpha) \tag{18}$$
$$d\cos\theta = 1 + \cos\alpha + \cos(\alpha' - \alpha) \tag{19}$$
$$d\sin\theta' = \sin\alpha' + \sin(\alpha' - \alpha) \tag{20}$$
$$d\cos\theta' = 1 + \cos\alpha' + \cos(\alpha' - \alpha) \tag{21}$$

Equation 17 is the second equation of System 13. We show how to compute the two other equations of System 13 for the possible orientations of X and X'.

• $\mathcal{P}$ has the same orientation on $\mathcal{X}$ and $\mathcal{C}$ (see Figure 15).
Let $\lambda = \angle(\overrightarrow{HO}, \overrightarrow{HI})$ and consider the triangle (OHI) :

$$\frac{\sin(\alpha + \varphi)}{2h} = \frac{\sin\lambda}{2}$$

As $\lambda = \alpha + \varphi - \theta - \omega\ [2\pi]$, we get :

$$h\sin(\alpha + \varphi - \theta - \omega) - \sin(\alpha + \varphi) = 0 \tag{22}$$

That equation can be expanded with respect to θ, and simplified thanks to Equations 18 and 19 :

$$h\sin(\varphi - \omega) + h\sin(\alpha' + \varphi - \omega) + h\sin(\alpha + \varphi - \omega) - d\sin(\alpha + \varphi) = 0 \tag{23}$$

• $\mathcal{P}$ has the same orientation on $\mathcal{X}'$ and $\mathcal{C}'$.
Similarly as above, we obtain the following equations :

$$h'\sin(\alpha' + \varphi' - \theta' - \omega') - \sin(\alpha' + \varphi') = 0 \tag{24}$$
$$h'\sin(\varphi' - \omega') + h'\sin(\alpha + \varphi' - \omega') + h'\sin(\alpha' + \varphi' - \omega') - d\sin(\alpha' + \varphi') = 0 \tag{25}$$

• $\mathcal{P}$ has opposite orientations on $\mathcal{X}$ and $\mathcal{C}$ (see Figure 16).

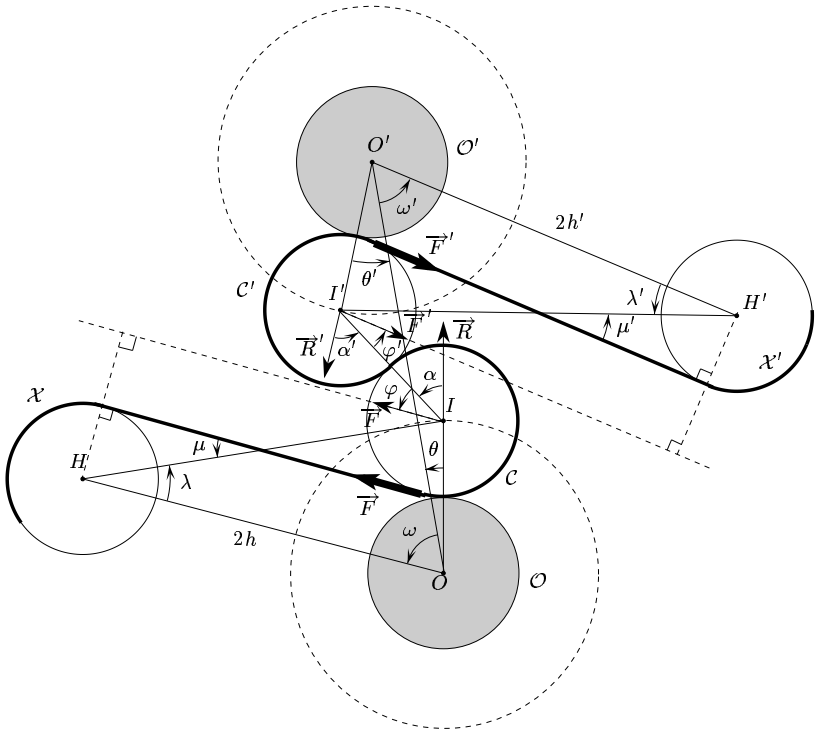

Figure 16: For the proof of Theorem 15 when both obstacle edges are circular edges

Let $\mu = \angle(\overrightarrow{F}, \overrightarrow{IH})$ and consider the triangle (OHI) :

$$\frac{\sin(\alpha+\varphi+\mu)}{2h} = \frac{\sin\lambda}{2} = \frac{\sin(\theta+\omega)}{IH}$$

As $\lambda = \alpha+\varphi+\mu-\theta-\omega\ [2\pi]$, we get :

$$\begin{aligned} 2\sin(\theta+\omega) &= IH\sin(\alpha+\varphi-\theta-\omega)\cos\mu + IH\cos(\alpha+\varphi-\theta-\omega)\sin\mu \\ 2h\sin(\theta+\omega) &= IH\sin(\alpha+\varphi)\cos\mu + IH\cos(\alpha+\varphi)\sin\mu \end{aligned}$$

Eliminating $\cos\mu$ from these two equations gives :

$$\begin{aligned} &2\sin(\theta+\omega)\sin(\alpha+\varphi) - 2h\sin(\theta+\omega)\sin(\alpha+\varphi-\theta-\omega) = \\ &\quad IH\cos(\alpha+\varphi-\theta-\omega)\sin\mu\sin(\alpha+\varphi) - IH\cos(\alpha+\varphi)\sin\mu\sin(\alpha+\varphi-\theta-\omega) \end{aligned}$$

We simplify this equation into :

$$2\sin(\theta+\omega)\sin(\alpha+\varphi) - 2h\sin(\theta+\omega)\sin(\alpha+\varphi-\theta-\omega) = IH\sin\mu\sin(\theta+\omega)$$

As $\sin\mu = 2/IH$ (see Figure 16), we have :

$$\sin(\theta+\omega)(h\sin(\alpha+\varphi-\theta-\omega) - \sin(\alpha+\varphi) + 1) = 0$$

We can assume that $\sin(\theta+\omega) \neq 0$ because otherwise I lies on the straight line OH and the number of such paths is less than four. Thus, the moving object is at an equilibrium only if :

$$h\sin(\alpha+\varphi-\theta-\omega) - \sin(\alpha+\varphi) + 1 = 0 \tag{26}$$

Similarly as above, we expand that equation with respect to θ and simplify it, thanks to Equations 18 and 19 :

$$h\sin(\varphi-\omega) + h\sin(\alpha'+\varphi-\omega) + h\sin(\alpha+\varphi-\omega) - d\sin(\alpha+\varphi) + d = 0 \tag{27}$$

- $\mathcal{P}$ have opposite orientations on $\mathcal{X}'$ and $\mathcal{C}'$.

Similarly as above, we obtain the following equations :

$$h'\sin(\alpha'+\varphi'-\theta'-\omega') - \sin(\alpha'+\varphi') + 1 = 0 \tag{28}$$

$$h'\sin(\varphi'-\omega') + h'\sin(\alpha+\varphi'-\omega') + h'\sin(\alpha'+\varphi'-\omega') - d\sin(\alpha'+\varphi') + d = 0 \tag{29}$$

That ends the proof of the lemma. □

We now show that System 13 has a finite number of roots $(\alpha, \alpha, \varphi, \varphi')$ (in $(S^1)^4$). It then follows that the moving object D has a finite number of equilibriums.

We expand each equation of System 13 and apply the variable substitution $x = \tan(\alpha/2)$, $y = \tan(\alpha'/2)$, $z = \tan(\varphi/2)$ and $t = \tan(\varphi'/2)$. This yields an algebraic system consisting of four equations where x, y, z, t are the four indeterminates and $\sin\omega$, $\cos\omega$, d, h, h', l' are considered as six independent parameters. Let $E_i = 0$ $(i \in \{1, \ldots, 4\})$ denote the algebraic equation obtained from the i-th equation of System 13. We compute[2] the resultant E_{14} of E_1 and E_4 with respect to the indeterminate t. E_{14} can be written as $16(1+y^2)E'_{14}$. We compute[3] the resultant Q

[2] We used AXIOM on a Sun Sparc-10 4 × 72Mhz with 512MB of main memory. Notice that several polynomials considered here are two big to be computed with MAPLE.

[3] This computation takes roughly eleven hours and the process exceeds 130MB.

of E'_{14} and E_2 with respect to the indeterminate y. We also compute the resultant T of E_2 and E_3 with respect to the indeterminate y. Q and T are two polynomials where x and z are the indeterminates.

Now, let R be the resultant of Q and T with respect to z. R is a uni-variate polynomial in the indeterminate x and we want to show that $R(x) \not\equiv 0$. Let

$$Q = q_0 + q_1\, z + \ldots + q_n\, z^n,\ q_n \neq 0,$$

$$T = t_0 + t_1\, z + \ldots + t_m\, z^m,\ t_m \neq 0,$$

where the q_i and the t_i are uni-variate polynomials in the variable x. The resultant R of Q and T with respect to z is the determinant of the $(n+m)\times(n+m)$ Sylvester matrix of Q and T with respect to z [3] :

$$R = \begin{vmatrix}
q_0 & q_1 & . & . & . & . & . & q_n & & & \\
 & q_0 & . & . & . & . & . & q_{n-1} & q_n & & \\
 & & . & . & . & . & . & . & . & . & \\
 & & & & q_0 & . & . & . & . & . & q_n \\
t_0 & t_1 & . & . & t_{m-1} & t_m & & & & & \\
 & . & . & . & . & . & . & . & . & & \\
 & & & & & & t_0 & . & . & . & t_m
\end{vmatrix}$$

The resultant $R(x)$ is too big to be computed with existing computer algebra systems but we are able to compute its leading monomial. The polynomials q_i appear in the first m rows of the Sylvester determinant and the polynomials t_i appear in the last n rows. Thus the degree of R with respect to x is at most

$$m \max_{i\in\{0,\ldots,n\}} degree(q_i(x)) + n \max_{i\in\{0,\ldots,m\}} degree(t_i(x)) = 168.$$

As existing computer algebra systems cannot compute the resultant R, we replace in the Sylvester determinant each $q_i(x)$ by its monomial of highest degree if $degree(q_i(x)) = \max_{i\in\{0,\ldots,n\}} degree(q_i(x))$ and by 0 otherwise, and each $t_i(x)$ by its monomial of highest degree if $degree(t_i(x)) = \max_{i\in\{0,\ldots,m\}}$
$degree(t_i(x))$ and by 0 otherwise. We then compute the determinant and obtain :

$$2^{56}\, d^8\, (d^2-1)^{32}\, h^{16}\, (h'^2 \sin^2\omega' + (h'\cos\omega' - d)^2)^4\, (d^2 h'^2 \sin^2\omega' + (dh'\cos\omega' - 1)^2)^4\, x^{168}$$

When this monomial is not zero, its degree is 168 and so it is the leading monomial of $R(x)$. Hence $R(x) \equiv 0$ only if $d = 1$ or $h = 0$ or $(\omega', h') = (0, d)$ or $(\omega', h') = (0, 1/d)$. $h \neq 0$ since, otherwise $\mathcal{P}$ is of type $X\bar{C}\bar{C}'SX'$ where X is a circular arc; the proof

of Theorem 9 shows that $\mathcal{P}$ is optimal only if either $\bar{C}$ or $\bar{C}'$ is anchored which contradicts the assumption made at the beginning of the proof. If $(\omega', h') = (0, d)$ or $(\omega', h') = (0, 1/d)$ we replace ω' and h' by their value in Q and T. Then, we apply the same procedure as above and show that the leading monomial of $R(x)$ is

$$2^{72}\, d^{16}\, (d^2-1)^{32}\, h^{16}\, x^{152}.$$

This leading monomial does not depend on whether $h' = d$ or $h' = 1/d$ and on the orientation of $\mathcal{P}$ on $\mathcal{X}$ and $\mathcal{X}'$. Since the obstacles are disjoint, $d \neq 1$ and $R(x) \not\equiv 0$ (in the case $d = 1$, it can also be shown that the number of roots of the system of equations is finite).

Hence, the number of roots of System 13 is finite since any given value of x determines at most two triplets of values for the other indeterminates y, z and t (see Figure 15). It follows that the number of possible equilibriums of our mechanical device is finite.

Case 3 : One obstacle edge is a line segment and the other is a circular arc

The proof is similar to the previous case. We assume, without loss of generality, that $\mathcal{O}$ and $\mathcal{O}'$ are respectively a circular edge and a line segment.

Let $\mathcal{D}'$ be the line parallel to $\mathcal{O}'$ passing through I' and oriented such that $\angle(\overrightarrow{R'}, \mathcal{D}') = -\pi/2$ (see Figure 17). Let O be the center of the circle (of unit radius) supporting $\mathcal{O}$. Let $\tilde{O}$ be the orthogonal projection of O onto $\mathcal{D}'$ and $2d$ the length of $O\tilde{O}$. Let $2h$ be the length of OH. Let $\tilde{H}'$ be the orthogonal projection of H' onto $\mathcal{D}'$. Let $2x'$ and $2l'$ be the algebraic lengths of $\tilde{O}I'$ and $\tilde{O}\tilde{H}'$ on the oriented line $\mathcal{D}'$. Let $2h'$ be the algebraic distance between H' and $\mathcal{D}'$ with $2h' > 0$ iff $\overrightarrow{\tilde{H}'H'}$ and $\overrightarrow{R'}$ have opposite orientations. Let $\omega = \angle(\overrightarrow{OO}, \overrightarrow{OH})$.

Lemma 19 *The moving object D is at an equilibrium only if :*

$$\begin{cases} \sin(\alpha'-\alpha) + \sin\alpha' \sin(\alpha+\varphi) - \sin\alpha \sin(\alpha'+\varphi') = 0 \\ \cos(\alpha'-\alpha) + \cos\alpha' = d \\ h\sin(\alpha'+\varphi-\omega) - \sin(\alpha+\varphi) + \delta = 0 \\ h'\sin(\alpha'+\varphi') + \cos(\alpha'+\varphi')\,(\sin\alpha' + \sin(\alpha'-\alpha) - l') + \delta' = 0 \end{cases} \tag{30}$$

where δ (resp. δ') is zero if the path $\mathcal{P}$ has the same orientation on $\mathcal{X}$ and $\mathcal{C}$ ($\mathcal{X}'$ and $\mathcal{C}'$) and 1 otherwise.

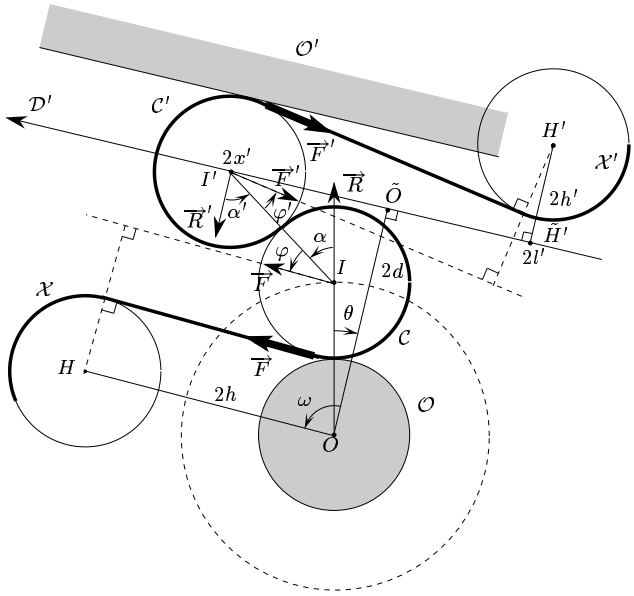

Figure 17: Mechanical device where one obstacle edge is a line segment and the other is a circular edge

Proof: The first equation of System 30 is given by Lemma 16. Now, let $\theta = \angle(\overrightarrow{OI}, \overrightarrow{OO})$. Considering the polygon $(OII'\tilde{O})$ in Figure 17, we have :

$$\begin{aligned}
&\alpha' = \alpha - \theta \ [2\pi] \\
&\cos\theta + \cos(\alpha - \theta) = d \\
&-\sin\theta + \sin(\alpha - \theta) = x'
\end{aligned}$$

Which gives :

$$\cos(\alpha' - \alpha) + \cos\alpha' = d \quad (31)$$

$$\sin(\alpha' - \alpha) + \sin\alpha' = x' \quad (32)$$

Equation 31 is the second equation of System 30. We show how to compute the two other equations of System 30 for each possible orientation of X and X'.

- If $\mathcal{P}$ has the same orientation on $\mathcal{X}$ and $\mathcal{C}$, then Equation 22 still holds :

$$h\sin(\alpha + \varphi - \theta - \omega) - \sin(\alpha + \varphi) = 0$$

Thus, as $\alpha' = \alpha - \theta\ [2\pi]$:

$$h\sin(\alpha' + \varphi - \omega) - \sin(\alpha + \varphi) = 0 \tag{33}$$

- If $\mathcal{P}$ has opposite orientations on $\mathcal{X}$ and $\mathcal{C}$, then Equation 26 still holds :

$$h\sin(\alpha + \varphi - \theta - \omega) - \sin(\alpha + \varphi) + 1 = 0$$

Thus, as $\alpha' = \alpha - \theta\ [2\pi]$:

$$h\sin(\alpha' + \varphi - \omega) - \sin(\alpha + \varphi) + 1 = 0 \tag{34}$$

- If $\mathcal{P}$ has the same orientation on $\mathcal{X}'$ and $\mathcal{C}'$, then Equation 7 still holds :

$$\tan(\alpha' + \varphi') = \frac{l' - x'}{h'}$$

By Equation 32, we obtain :

$$h'\sin(\alpha' + \varphi') + \cos(\alpha' + \varphi')\,(\sin\alpha' + \sin(\alpha' - \alpha) - l') = 0 \tag{35}$$

- If $\mathcal{P}$ has opposite orientations on $\mathcal{X}'$ and $\mathcal{C}'$, then Equation 11 still holds :

$$(x' - l')\cos(\alpha' + \varphi') + h'\sin(\alpha' + \varphi') = -1$$

Using Equation 32, we get :

$$h'\sin(\alpha' + \varphi') + \cos(\alpha' + \varphi')\,(\sin\alpha' + \sin(\alpha' - \alpha) - l') + 1 = 0 \tag{36}$$

That ends the proof of the lemma. □

We now show that System 30 has a finite number of roots $(\alpha, \alpha, \varphi, \varphi')$ (in $(S^1)^4$). We consider the variable substitution $x = \tan(\alpha/2)$, $y = \tan(\alpha'/2)$, $z = \tan(\varphi/2)$ and $t = \tan(\varphi'/2)$, and we apply exactly the same procedure as in Case 2, except that $E'_{14} = E_{14}/16(1 + y^2)^2$. It follows that the leading monomial of $R(x)$ is

$$2^{64}\, d^{32}\, h^{16}\, (l'^2 + (h' - d)^2)^4\, (l'^2 + (h' + d)^2)^4\, x^{176}.$$

This leading monomial does not depend on the orientation of $\mathcal{P}$ on $\mathcal{X}$ and $\mathcal{X}'$. Hence the polynomial $R(x) \equiv 0$ only if $h = 0$ or $(l', h') = (0, \pm d)$. As above, we can eliminate the case $h = 0$ and if $(l', h') = (0, d)$ or $(l', h') = (0, -d)$ we replace l' and h' by their value in Q and T. In both cases, the leading monomial of $R(x)$ becomes :

$$2^{80}\, d^{32}\, h^{16}\, x^{160}.$$

This leading monomial does not depend on the orientation of $\mathcal{P}$ on $\mathcal{X}$ and $\mathcal{X}'$. Thus we have shown that $R(x) \not\equiv 0$. It follows that the number of roots of System 30 is finite because any given value of x determines at most two triplets of values for the other indeterminates y, z and t (see Figure 17). Therefore, the number of possible equilibriums of our mechanical device is finite.

That ends the proof of Theorem 15.

Remark 20 Although the degree of $R(x)$ is very large in Cases 2 and 3, we can prove that the number of potential equilibriums of the mechanical device is much smaller. Indeed, let S be an algebraic system of n equations in n indeterminates. It is well known that the number of complex roots of S is either infinite or less or equal to the generic number of roots, *i.e.* the number of roots for a generic[4] choice of the parameters. Moreover, the set of parameters for which the number of roots of S is not equal to the generic number of roots is included in an algebraic set, and thus is of measure 0. The algebraic systems under consideration in Cases 1, 2 and 3 have the same number of equations and indeterminates and we have shown that the number of roots of these systems is finite for any choice of the parameters. It follows that the number of roots of these systems are, with probability 1, maximal for a random choice of the parameters. In order to estimate the number of solutions of our systems, we use Gröbner basis and compute the number of roots for some pseudo random choices of the parameters. In this way, we obtain that the maximal number of roots of System 13 is 36, with probability close to 1, instead of $336 = 2\,.\,degree(R(x))$.

6 The algorithm

Let $\mathcal{O}_1, \ldots, \mathcal{O}_m$ be the disjoint moderate obstacles. We denote by $\mathcal{S}_O$ the set of the obstacle edges and by n its size.

Let S and F be the initial and the final point of the optimal path that we want to compute. By Theorems 9 and 10, any C-segment is either an anchored C-segment, or is adjacent to a terminal C-segment and to an anchored C-segment, or belongs to a subpath of type $XS\bar{C}\bar{C}SX'$ where $X, X' \in \{O, \bar{\bar{C}}\}$ (the lengths of the S-segments being possibly zero).

The algorithm computes first the set $\mathcal{S}_{\bar{\bar{C}}}$ of all the maximal free anchored arcs of circle. A *maximal free anchored arc* is a maximal arc of an anchored circle that does not intersect the interior of the obstacles. It will be simply called a free anchored

[4] A choice of the parameters is called generic if the values of the parameters do not satisfy any algebraic relation other than those of the system.

arc in the sequel. We will also say for short that an arc (or a subpath) intersects an obstacle iff it intersects the interior of the obstacle.

To each obstacle and for a given r, we associate a *grown obstacle* which is the Minkowski sum of the obstacle and of a disk of radius r. Let $\mathcal{A}_r$ be the arrangement of the boundaries of these grown obstacles. A point is said of *level* i in $\mathcal{A}_r$ if it belongs to the interior of i grown obstacles. The vertices of level 0 are simply the vertices of the boundary of the union of the grown obstacles. Because the obstacles are disjoint, there are $O(n)$ such vertices by a result of Kedem et al. [13]. The same bound holds for the number of vertices of the k first levels for any constant k by the random sampling theorem of Clarkson and Shor [8].

Lemma 21 *The number of free anchored arcs is $O(n)$ and these arcs can be computed in $O(n \log n)$ time.*

Proof: A circle of unit radius is intersected by at most five obstacles. Indeed, the obstacles are disjoint and moderate which implies that each one contains a circle of unit radius. The claim follows since there are at most five pairwise disjoint circles of unit radius that may intersect a given circle of unit radius. It follows that any point is of level at most five in $\mathcal{A}_1$. Hence, $\mathcal{A}_1$ has linear size and can be computed in $O(n \log n)$ time by standard techniques.

Since the centers of the anchored circles are the vertices of $\mathcal{A}_1$ and each anchored circle is intersected by at most five obstacles, the lemma is proved. □

Once the free anchored arcs have been computed, we compute the set $\mathcal{S}_S$ of all the free line segments that are tangent to two arcs of $\mathcal{S}_{\bar{C}} \cup \mathcal{S}_O$.

Lemma 22 *$\mathcal{S}_S$ has size $O(n^2)$ and can be computed in $O(n^2 \log n)$ time.*

Proof: First, we compute all the free line segments tangent to two obstacles. Let us consider each obstacle in turn, say $\mathcal{O}_1$ for concreteness. Let D_θ be an oriented line of orientation θ tangent to $\mathcal{O}_1$. The set of common points between $\mathcal{O}_1$ and D_θ is either a single point or a line segment; let P_θ be either this single point or the middle point of the line segment. If D_θ intersects $\mathcal{O}_i$ $(i = 2, \ldots, m)$, we call P_i the point common to D_θ and $\mathcal{O}_i$ that is closer to P_θ. Let $f_i(\theta)$ be the algebraic length of $P_\theta P_i$ on the oriented line D_θ.

Let $\mathcal{E}^+$ (resp. $\mathcal{E}^-$) be the lower (upper) envelope of the functions f_i that are positive (negative). As the obstacles are pairwise disjoint, $f_i(\theta) \neq 0$ and $f_i(\theta) \neq f_j(\theta)$ for all θ and $i \neq j$. It follows that $\mathcal{E}^+$ and $\mathcal{E}^-$ can be computed in $O(n \log n)$ time. A line segment joining P_θ to P_i is free iff $(\theta, f_i(\theta))$ belongs to $\mathcal{E}^+$ or $\mathcal{E}^-$. Moreover,

a line segment $P_\theta P_i$ is tangent to $\mathcal{O}_i$ iff P_i is an end-point of f_i. Hence, computing the free line segments tangent to $\mathcal{O}_1$ and another obstacle reduces to compute $\mathcal{E}^+$ and $\mathcal{E}^-$.

Repeating the above procedure for all the obstacles, we conclude that all the free line segments tangent to two obstacles can be computed in $O(n^2 \log n)$ time.

We now compute the free line segments tangent to a free anchored arc and to either an obstacle or another anchored free arc. Let $C_1, \ldots, C_p$ be the anchored free arcs. We consider in turn each free anchored arc, say C_1 for concreteness, and apply exactly the same procedure as above to compute the free line segments tangent to C_1 and to an obstacle. As above, these segments can be computed in $O(n \log n)$ time by computing the envelopes $\mathcal{E}^+$ and $\mathcal{E}^-$. It remains to compute the free line segments tangent to C_1 and to the other anchored free arcs $C_2, \ldots, C_p$. We define a function g_i involving C_1 and C_i and similar to the function f_i defined above. To each end point of g_i that lies between $\mathcal{E}^+$ and $\mathcal{E}^-$ corresponds a free line segment tangent to C_1 and C_i. Deciding if such an end point lies between $\mathcal{E}^+$ and $\mathcal{E}^-$ can be done in $O(\log n)$ time by binary search once the envelopes have been computed. As the number of free anchored arcs is $O(n)$ by Lemma 21, the free line segments tangent to C_1 and to another anchored free arc can be computed in $O(n \log n)$ time. Hence, the free line segments tangent to an anchored free arc and to either an obstacle or another anchored free arc can be computed in $O(n^2 \log n)$ time in total.

This achieves the proof. □

We consider now the subpaths of type $C_t C \bar{\bar{C}}$ and $\bar{\bar{C}} C C_t$. We compute the set $\mathcal{S}_C$ of all the circular arcs that avoid the obstacles and are tangent to a terminal circle and to an anchored free arc. As there are $O(n)$ anchored free arcs, this step can easily be done in $O(n^2)$ time.

By Theorem 9, $\mathcal{S}_{\bar{C}} \cup \mathcal{S}_O \cup \mathcal{S}_S \cup \mathcal{S}_C$ contains all the arcs potentially taken by an optimal path except the subpaths of type $XS\bar{C}\bar{C}SX'$. We consider, in turn, all the quadruplets $(\mathcal{X}, \mathcal{O}, \mathcal{O}', \mathcal{X}')$ where $\mathcal{X}$ and $\mathcal{X}'$ are obstacle edges or anchored arcs, and where $\mathcal{O}$ and $\mathcal{O}'$ are two obstacle edges. First, we compute the family of potential optimal subpaths of type $XS\bar{C}\bar{C}SX'$ where X (resp. X') is an arc of $\mathcal{X}$ ($\mathcal{X}'$) and the two C-segments $\bar{C}\bar{C}$ are respectively tangent to $\mathcal{O}$ and $\mathcal{O}'$. In a second step, we will check whether or not these potential optimal subpaths intersect other obstacles.

By solving an algebraic system as described in the proof of Theorem 15, we compute the family of potential optimal subpaths of type $XS\bar{C}\bar{C}SX'$ when neither of the two C-segments, tangent to $\mathcal{O}$ and $\mathcal{O}'$ respectively, is anchored. That step can be performed in constant time for each chosen quadruplet assuming that the roots of a polynomial of bounded degree can be computed in constant time. Hence the

total time complexity of this step is $O(n^4)$. We also compute the subpaths of type $XS\bar{\bar{C}}\bar{C}SX'$ and $XS\bar{C}\bar{\bar{C}}SX'$. As the number of anchored C-segments is $O(n)$, the total number of these subpaths is $O(n^4)$ and they can be easily computed in $O(n^4)$ time. It remains to compute the set $\mathcal{S}_{\bar{C}\bar{C}}$ of those subpaths that avoid the obstacles.

Lemma 23 *$\mathcal{S}_{\bar{C}\bar{C}}$ can be computed in $O(n^4 \log n)$ time.*

Proof: We show that we can check in $O(\log n)$ time whether or not a given subpath of type $XS\bar{C}\bar{C}SX'$ intersects the obstacles. We consider successively the case of an arc of circle and the case of a line segment.

As mentioned in the proof of Lemma 21, a circle of unit radius intersects at most five obstacles. We can identify the obstacles that intersect the circle supporting a given arc $\bar{C}$ by locating in $O(\log n)$ time the center of this circle in the arrangement $\mathcal{A}_1$. It then remains to check if the arc $\bar{C}$ (not the whole circle) actually intersects one of the obstacles. Each such test can be done in $O(\log n)$ time since each obstacle has $O(n)$ edges [9].

We describe now how to check if a line segment S of a subpath of type $XS\bar{C}\bar{C}SX'$ intersects the obstacles. By Lemma 11, the length of S is at most 4. It follows that if S intersects an obstacle, each of its end points are contained in the obstacle grown by a disk of radius 4. As the obstacles are disjoint and moderate, a point can only be contained in $g = O(1)$[5] such grown obstacles; hence, arrangement $\mathcal{A}_4$ has linear size and can be computed in $O(n \log n)$ time. We locate one endpoint of S in $\mathcal{A}_4$ and find the at most g obstacles that may intersect S. We consider in turn each of these obstacles and check if S indeed intersects the obstacle. This can be done in $O(\log n)$ time [9]. □

By Theorems 9, $\mathcal{S}_{\bar{\bar{C}}} \cup \mathcal{S}_O \cup \mathcal{S}_S \cup \mathcal{S}_C \cup \mathcal{S}_{\bar{C}\bar{C}}$ contains all the arcs potentially taken by an optimal path.

Let $\mathcal{G}$ be the weighted graph whose nodes are the tangent points between two arcs of $\mathcal{S}_{\bar{\bar{C}}} \cup \mathcal{S}_O \cup \mathcal{S}_S \cup \mathcal{S}_C \cup \mathcal{S}_{\bar{C}\bar{C}}$ and whose edges are the arcs of $\mathcal{S}_{\bar{\bar{C}}} \cup \mathcal{S}_O \cup \mathcal{S}_S \cup \mathcal{S}_C \cup \mathcal{S}_{\bar{C}\bar{C}}$. The final step of the algorithm consists in searching a shortest path in this graph.

Theorem 24 *An optimal path amidst a set of disjoint moderate obstacles with n edges in total can be computed in $O(n^4 \log n)$ time.*

[5] g is the maximal number of disjoint disks of unit radius that can be packed in a disk of radius 6.

Improving the performances of the algorithm

We now show that the time complexity of the algorithm can be reduced in most practical situations. This is a consequence of the fact that the subpaths of type $\bar{C}\bar{C}$ can only be encountered near the endpoints of the path. Proposition 25 is a consequence of a claim of Agarwal et al. [1]. We give here a complete proof.

Proposition 25 *Let $\mathcal{P}$ be an optimal path consisting of four parts $\mathcal{P}_1$, $\mathcal{P}_2$, $\mathcal{P}_3$ and $\mathcal{P}_4$ in this order where $\mathcal{P}_2$ and $\mathcal{P}_3$ are C-segments. Let $\mathcal{C}_2$ and $\mathcal{C}_3$ be the circles supporting $\mathcal{P}_2$ and $\mathcal{P}_3$, and let O_2 and O_3 be their centers.*

1. *If $\mathcal{C}_3$ is not obstructed by any obstacle or if $\mathcal{C}_2$ is obstructed by an obstacle, then for any M on $\mathcal{P}_1$, the Euclidean distance between M and O_3 is smaller than 3.*
2. *If $\mathcal{C}_3$ is obstructed by an obstacle or if $\mathcal{C}_2$ is not obstructed by any obstacle, then for any M on $\mathcal{P}_4$, the Euclidean distance between M and O_2 is smaller than 3.*

Proof: We only prove the first claim; the second one is symmetrical. We assume, without loss of generality, that $\mathcal{P}_2$ and $\mathcal{P}_3$ are oriented counterclockwise and clockwise respectively.

We recall some notations indroduced in Section 2 : let M be a point of $\mathcal{P}$ and let $C_L(M)$ (resp. $C_R(M)$) be the unit circle tangent to $\mathcal{P}$ at M and lying on the left (resp. right) side of the path $\mathcal{P}$ oriented from S to T. $C_L(M)$ is oriented counterclockwise and $C_R(M)$ is oriented clockwise. An arc of one of these circles will be oriented accordingly.

We show that for any M on $\mathcal{P}_1$, $C_L(M)$ intersects $\mathcal{C}_3$. It will immediately follow that the Euclidean distance between M and O_3 is smaller than 3.

Suppose for a contradiction that there exists M on $\mathcal{P}_1$ such that $C_L(M)$ does not intersect $\mathcal{C}_3$. Let M_0 be the point of $\mathcal{P}_1$ such that for any point M located after M_0 on the relative interior of $\mathcal{P}_1$, $C_L(M)$ properly intersects $\mathcal{C}_3$ (see Figure 18); M_0 exists because $\mathcal{P}_2$ is greater than π by Lemma 5. Let M_1 be the common point to $C_L(M_0)$ and $\mathcal{C}_3$, and M_2 be the common end point of $\mathcal{P}_2$ and $\mathcal{P}_3$.

We distinguish whether $M_1 \in \mathcal{P}_3$ or not. In each case we show that the dashed path of Figure 18 shortens $\mathcal{P}$ and avoids all the moderate obstacles, which contradicts the fact that $\mathcal{P}$ is optimal.

Case 1 : $M_1 \in \mathcal{P}_3$.

We first show that the arc $[M_0M_1]$ of $C_L(M_0)$ is not obstructed by any moderate obstacle. A disk of unit radius that intersects $[M_0M_1]$ without intersecting the portion $\mathcal{P}(M_0, M_1)$ of $\mathcal{P}$ between M_0 and M_1 is included in the region $\mathcal{R}$ inside

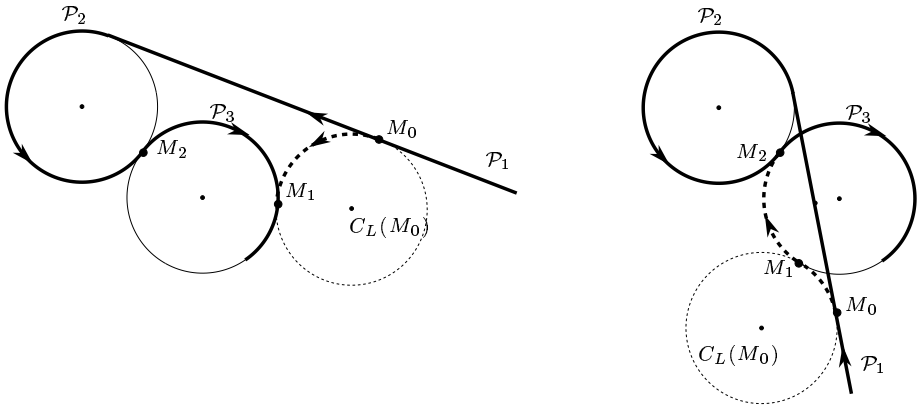

Figure 18: Shortcuts in the proof of Proposition 25

the closed curve that is the concatenation of $\mathcal{P}(M_0, M_1)$ and of the arc $[M_1M_0]$ of $C_L(M_0)$ (see Figure 19). By the definition of M_0, the relative interior of the arc of $\mathcal{P}_1$ located after M_0 is strictly included in the disk of radius 3 centered at O_3. It follows that the only disks of unit radius included in $\mathcal{R}$ are the disks whose boundaries are $\mathcal{C}_2$ and $C_L(M_0)$ (which may possibly intersect). Since $\mathcal{P}_2$ is not an arc of the boundary of the obstacles by hypothesis, $[M_0M_1]$ is not obstructed by any moderate obstacle.

By the definition of M_0, $[M_0M_1]$ is smaller than π and so shortens $\mathcal{P}$ because $\mathcal{P}_2$ is strictly greater than π.

Case 2 : $M_1 \notin \mathcal{P}_3$**.**

First notice that the circle $\mathcal{C}_2$ is not obstructed by any obstacle. Indeed, otherwise M_0 must lie in the hashed region of Figure 20a and, as $\mathcal{P}_3$ is greater than π, $M_1 \in \mathcal{P}_3$ which contradicts the hypothesis. By the hypothesis of the first claim of the proposition, it follows that $\mathcal{C}_3$ is not obstructed by any obstacle. That implies that the arc $[M_0M_1]$ of $C_L(M_0)$ avoids all the moderate obstacles because otherwise, the portion of $\mathcal{P}$ between M_0 and M_2 cannot lie entirely in the disk of radius 3 centered at O_3 (see Figure 20b), which contradicts the definition of M_0. Hence, the concatenation of the arc $[M_0M_1]$ of $C_L(M_0)$ and the arc $[M_1M_2]$ of $\mathcal{C}_3$ avoids all the moderate obstacles.

Moreover, the concatenation of $[M_0M_1]$ and $[M_1M_2]$ shortens $\mathcal{P}$. Indeed, the arc $[M_0M_1]$ is smaller than π by the definition of M_0, and, the arc $[M_1M_2]$ is smaller than π because $M_1 \notin \mathcal{P}_3$ and $\mathcal{P}_3$ is greater than π. It can be easily shown that

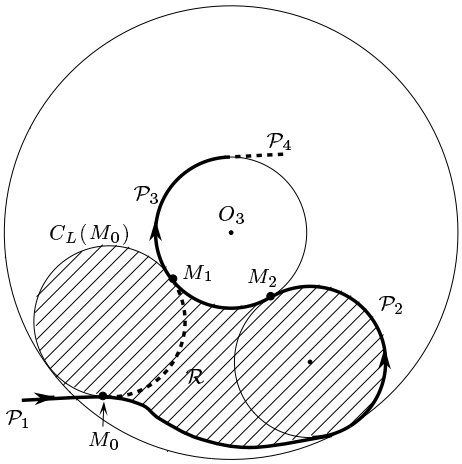

Figure 19: For the proof of Proposition 25 (Case 1)

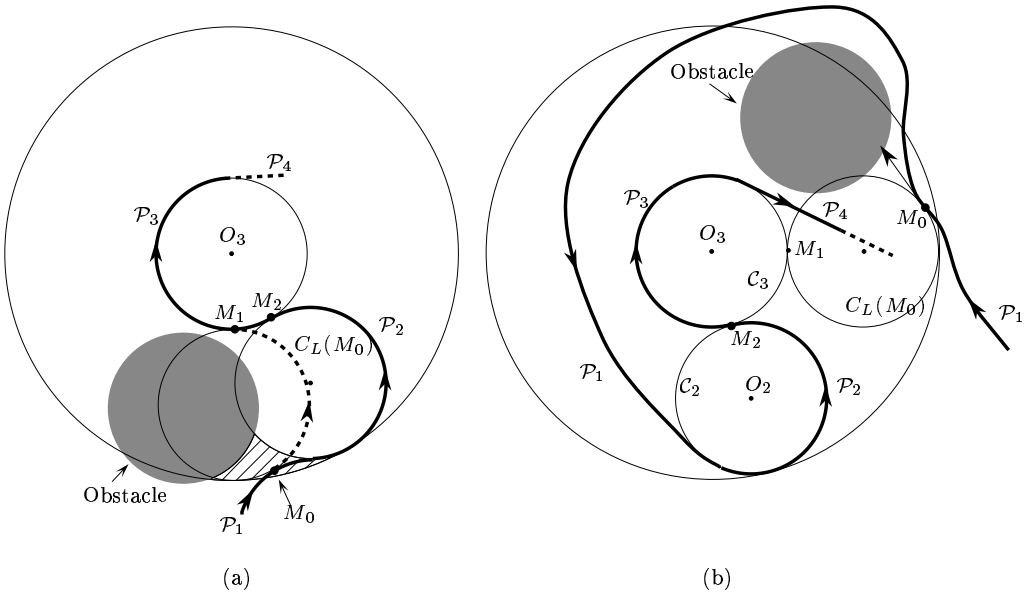

Figure 20: For the contradictions in the proof of Proposition 25 (Case 2)

the concatenation of two circular arcs of unit radius whose lengths are smaller than

π is a shortest path of bounded curvature (even if there is no obstacle). Hence, the concatenation of the arcs $[M_0M_1]$ and $[M_1M_2]$ shortens $\mathcal{P}$ and avoids all the moderate obstacles which contradicts the hypothesis that $\mathcal{P}$ is optimal. □

Remark 26 The previous proof yields that an optimal path contains at most two non-terminal $\bar{C}\bar{C}$-subpaths (i.e. subpaths of type $\bar{C}\bar{C}$ where both $\bar{C}$-segments are not terminal). For details see [1].

Theorem 27 *Let $\mathcal{P}$ be an optimal path joining S to F. Any subpath of $\mathcal{P}$ of type $XS\bar{C}\bar{C}SX'$, where $X, X' \in \{O, \bar{\bar{C}}\}$, is contained in one of the two disks of radius 9 centered at S or F.*

Proof: This theorem follows from Proposition 25 and we use the notations introduced in that proposition. Let $\mathcal{P}_1$ (resp. $\mathcal{P}_4$) be the portion of $\mathcal{P}$ between S (resp. F) and the first (resp. last) $\bar{C}$ in the considered subpath. From Proposition 25, we have $\forall M \in \mathcal{P}_1\ MO_3 \leq 3$ or $\forall M \in \mathcal{P}_4\ MO_2 \leq 3$. Assume without loss of generality that $\forall M \in \mathcal{P}_1\ MO_3 \leq 3$. Then, the starting point S and the whole subpath $XS\bar{C}\bar{C}$ is included in the disk of radius 3 centered at O_3 (see Figure 21).

On the other hand, by Lemma 11, the length of the line segment preceding X' is smaller than 4. Therefore, S and the whole subpath $XS\bar{C}\bar{C}SX'$ is included in a disk of diameter $3 + 2\sqrt{5} + 1 < 9$ (see Figure 21). Hence the subpath of type $XS\bar{C}\bar{C}SX'$ is included in a disk of radius 9 centered at S. □

According to Theorem 27, we can improve the procedure that computes the subpaths of type $XS\bar{C}\bar{C}SX'$. Indeed, instead of considering all n^4 quadruplets $(\mathcal{X}, \mathcal{O}, \mathcal{O}', \mathcal{X}')$, we can only consider those that intersect one of the disks of radius 9 centered at S and F. If k is the number of such quadruplets, the time complexity of the algorithm becomes $O(n^2 \log n + k^4 \log k)$. In particular, if the length of any obstacle edge is bounded from below by some positive constant, then $k = O(1)$.

Theorem 28 *Given a set of disjoint moderate obstacles with n edges whose lengths are bounded from below by some positive constant. An optimal path between two configurations amidst those obstacles can be computed in $O(n^2 \log n)$ time.*

7 Final remarks and open questions

The geometric results and the algorithm hold even if the obstacles are not disjoint. However, the time-complexity increases since the number of anchored C-segments may be not linear.

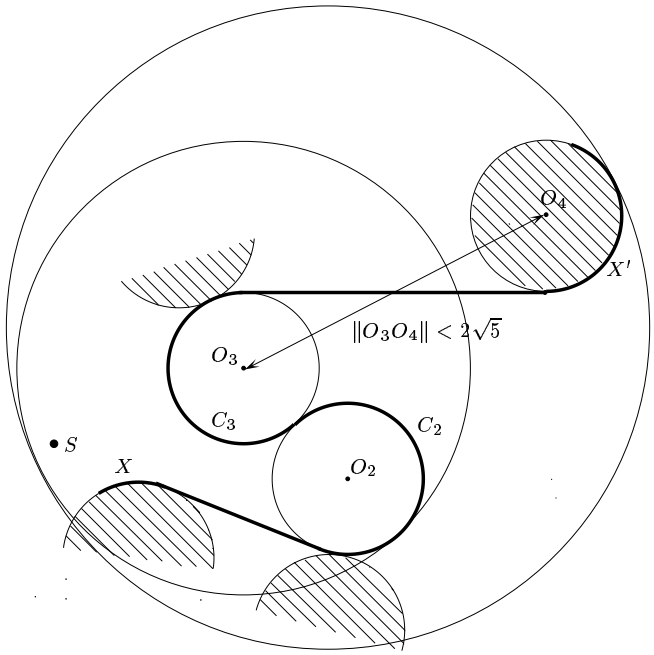

Figure 21: For the proof of Theorem 27

In this paper, we have considered obstacles whose boundaries consist of line segments and circular arcs of unit radius. Such obstacles can be obtained as the convex hull of bounded curvature of polygonal obstacles (see [6]). However, it would be interesting to consider more general moderate obstacles (in the sense of Agarwal et al.) and, in particular, obstacles whose boundaries consist of line segments and circular arcs of radii greater than or equal to 1. The system of equations corresponding to the equilibriums of the mechanical device (see Section 5) is very similar to the one in Lemma 18. However, the computations exceed the capabilities of the current computer algebra systems[6] and we have not been able to apply techniques similar to those of Section 5.

Many other questions remain open. We mention two of them we plan to consider in near future : Can similar results be obtained for polygonal robots? Can similar

[6]Using AXIOM, the size of the process exceeds 500MB.

results be obtained if backwards moves are allowed? (preliminary results in that direction can be found in [1, 5, 17]).

Acknowledgments : The authors would like to thank the GDR MEDICIS (GDR CNRS 1026) for giving them the oportunity to use the machines of the GAGE group at Ecole Polytechnique.

References

[1] P. K. Agarwal, P. Raghavan, and H. Tamaki. Motion planning for a steering-constrained robot through moderate obstacles. In *Proc. 27th Annu. ACM Sympos. Theory Comput.*, pages 343–352, 1995.

[2] J. Barraquand and J-C. Latombe. Nonholonomic multi-body mobile robots : controllability and motion planning in the presence of obstacles. *Algorithmica*, 10:121–155, 1993.

[3] Behnke, Bachmann, and Fladt. *Fundamentals of mathematics, Geometry*, volume 1. MIT Press, 1986.

[4] J-D. Boissonnat and X-N. Bui. Accessibility region for a car that only moves forwards along optimal paths. Research Report 2181, INRIA, BP93, 06902 Sophia-Antipolis, France, 1994.

[5] J.-D. Boissonnat, A. Cérézo, and J. Leblond. Shortest paths of bounded curvature in the plane. *Internat. J. Intell. Syst.*, 10:1–16, 1994.

[6] J-D. Boissonnat and S. Lazard. Convex hulls of bounded curvature. Research Report to appear, INRIA, BP93, 06902 Sophia-Antipolis, France, 1996.

[7] X-N. Bui, P. Souères, J-D. Boissonnat, and J-P. Laumond. Shortest path synthesis for Dubins non-holonomic robot. In *IEEE Int. Conf. on Robotics and Automation*, pages 2–7, San Diego, 8-13 Mai 1994.

[8] K. L. Clarkson and P. W. Shor. Applications of random sampling in computational geometry, II. *Discrete Comput. Geom.*, 4:387–421, 1989.

[9] D. P. Dobkin and D. L. Souvaine. Computational geometry in a curved world. *Algorithmica*, 5:421–457, 1990.

[10] L. E. Dubins. On curves of minimal length with a constraint on average curvature and with prescribed initial and terminal positions and tangents. *Amer. J. Math.*, 79:497–516, 1957.

[11] S. Fortune and G. Wilfong. Planning constrained motion. *Annals of Mathematics and Artificial Intelligence*, 3:21–82, 1991.

[12] P. Jacobs and J. Canny. Planning smooth paths for mobile robots. In *Proc. IEEE Internat. Conf. Robot. Autom.*, pages 2–7, 1989.

[13] K. Kedem, R. Livne, J. Pach, and M. Sharir. On the union of Jordan regions and collision-free translational motion amidst polygonal obstacles. *Discrete Comput. Geom.*, 1:59–71, 1986.

[14] J.-C. Latombe. *Robot Motion Planning.* Kluwer Academic Publishers, Boston, 1991.

[15] J-P. Laumond, M. Taix, P. Jacobs, and R.M. Murray. A motion planner for nonholonomic mobile robots. *IEEE Trans. on Robotics and Automation*, 1993.

[16] Z. Li and J.F. Canny. *Nonholonomic Motion Planning.* Kluwer Academic Publishers, 1992.

[17] J. A. Reeds and L. A. Shepp. Optimal paths for a car that goes both forwards and backwards. *Pacific Journal of Mathematics*, 145(2), 1990.

[18] H. J. Sussmann and G. Tang. Shortest paths for the reeds-shepp car: a worked out example of the use of geometric techniques in nonlinear optimal control. Research Report SYCON-91-10, Rutgers University, New Brunswick, NJ, 1991.

[19] H. Wang and P.K. Agarwal. Approximation algorithms for curvature constrained shortest paths. In *Proc. 7th ACM-SIAM Sympos. Discrete Algorithms (SODA '96)*, 1996.

Unité de recherche INRIA Lorraine, Technopôle de Nancy-Brabois, Campus scientifique,
615 rue du Jardin Botanique, BP 101, 54600 VILLERS LÈS NANCY
Unité de recherche INRIA Rennes, Irisa, Campus universitaire de Beaulieu, 35042 RENNES Cedex
Unité de recherche INRIA Rhône-Alpes, 46 avenue Félix Viallet, 38031 GRENOBLE Cedex 1
Unité de recherche INRIA Rocquencourt, Domaine de Voluceau, Rocquencourt, BP 105, 78153 LE CHESNAY Cedex
Unité de recherche INRIA Sophia-Antipolis, 2004 route des Lucioles, BP 93, 06902 SOPHIA-ANTIPOLIS Cedex

Éditeur
INRIA, Domaine de Voluceau, Rocquencourt, BP 105, 78153 LE CHESNAY Cedex (France)
ISSN 0249-6399